Semi-leptonic W decay to B meson with lepton pairs in HQET factorization upto $\mathcal{O}(\alpha_s)$

By

Sajawal Zafar

(Registration No: 00000364964)

A thesis submitted to the National University of Sciences and Technology, Islamabad,

in partial fulfillment of the requirements for the degree of

Master of Science in

Physics

Supervisor: Dr. Saadi Ishaq

School of Natural Sciences

National University of Sciences and Technology (NUST)

Islamabad, Pakistan

(2024)

THESIS ACCEPTANCE CERTIFICATE

Certified that final copy of MS thesis written by **Sajawal Zafar** (Registration No. **00000364964**), of **School of Natural Sciences** has been vetted by undersigned, found complete in all respects as per NUST statutes/regulations, is free of plagiarism, errors, and mistakes and is accepted as partial fulfillment for award of MS/M.Phil degree. It is further certified that necessary amendments as pointed out by GEC members and external examiner of the scholar have also been incorporated in the said thesis.
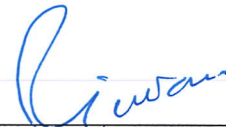
Signature: _____
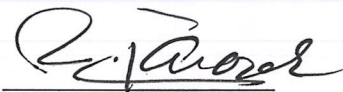
Name of Supervisor: Dr. Saadi Ishaq_____

Date: ___13/06/24_____

Signature (HoD): _____

Date: _____17-06-2024_____
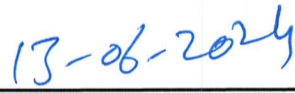
Signature (Dean/Principal): _____

Date: _____14.6.2024_____

National University of Sciences & Technology

MS THESIS WORK

We hereby recommend that the dissertation prepared under our supervision by: **"Sajawal Zafar"** Regn No. **00000364964** Titled: **"Semi-leptonic W Decay to B Meson with Lepton Pairs in HQET Factorization up to O(αs)"** accepted in partial fulfillment of the requirements for the award of **MS** degree.

Examination Committee Members

1.   Name: DR. MUHAMMAD ALI PARACHA   Signature:

2.   Name: DR. FAISAL MUNIR BHUTTA   Signature:

Supervisor's Name: DR. SAADI ISHAQ   Signature:

_____   13-06-2024
Head of Department   Date

COUNTERSINGED

Date: 14·6·2024   Dean/Principal

DEDICATION

"To my family, whose love and encouragement have been my constant source of strength throughout this journey. To my mentor and advisor, whose guidance and wisdom have shaped my scholarly path. To my friends and loved ones, for their unwavering support and understanding during times of challenge and triumph. And to all those who have inspired me along the way, this thesis is dedicated to you, with deep appreciation for your influence on my academic pursuits."

ACKNOWLEDGEMENTS

Contents

III

List of Tables

List of Figures

Abstract

We extend the factorization formalism for a somewhat complex process $W^+ \to B^+ \ell^+ \ell^-$ in the non-zero limit of invariant squared-mass of dilepton, q^2, at the lowest order in $1/m_b$ up to $\mathcal{O}(\alpha_s)$, inspired by the investigation of heavy-light meson production within the context of heavy quark effective theory (HQET) factorization. In current study, we have extended the HQET factorization formula for the decay $W^+ \to B^+ \ell^+ \ell^-$ and calculated the form factors up to next-to-leading order (NLO) corrections in α_s. We have shown that the amplitude of decay $W^+ \to B^+ \ell^+ \ell^-$ can be written into a convolution between the perturbatively calculable hard-scattering kernel and the non-perturbative light-cone distribution amplitude (LCDA) defined in HQET. The validity of HQET factorization depends on the assumed scale hierarchy $m_W \sim m_b \gg \Lambda_{\mathrm{QCD}}$. We calculated the form factors associated to $W^+ \to B^+ \ell^+ \ell^-$ process in HQET factorization, revealing details on its phenomenology. Furthermore, we conduct an exploratory phenomenological investigation on $W^+ \to B^+ \ell^+ \ell^-$ by using the LCDAs with an exponential model for B^+ meson. According to our research, the branching ratio for $W^+ \to B^+ \ell^+ \ell^-$ is below 10^{-10}. This channel in high luminosity LHC experiments may serve to further restrict the value of λ_B even when the branching ratios are small.

Chapter 1

Introduction

Standard Model of particle physics is the mathematical framework which describes the strong, electroweak and electromagnetic interactions between the leptons, quarks and fundamental particles of Standard Model. It is the result of an immense theoretical and experimental effort of nearly fifty years. Although it is the most well tested theory of particle physics, but data from several laboratories show deviation from the predictions of the SM. To improve the Standard Model, heavy flavour physics specially B-Physics provides a vital opportunity. CP violation and CKM matrices are the interesting areas of flavour physics which are not tested with high precision under the SM. CKM matrices dictate the degree of mixing the quarks mass and weak eigen states in weak interactions. The weak eigen states are related to mass eigen states by CKM matrix

$$
\begin{pmatrix} d' \\ s' \\ b' \end{pmatrix} = \begin{pmatrix} V_{ud} & V_{us} & V_{ub} \\ V_{cd} & V_{cs} & V_{cb} \\ V_{td} & V_{ts} & V_{tb} \end{pmatrix} \begin{pmatrix} d \\ s \\ b \end{pmatrix}. \tag{1.1}
$$

The numerical values of CKM matrices are calculated experimentally and it is still a challenge to precisely pin down their values. CP violation is another problem in particle physics which was first observed in 1964 while studying the neutral K-mesons. Later on, it was also observed and studied in detail in neutral B-mesons.

Weak decays are the most direct ways to find out the angles of CKM matrix and to test the flavour sector of SM. On the other side, these transition are important to study the non-perturbative part of the strong interactions.

Among the decays of B mesons, the exclusive B-decays in particular not only offer an excellent laboratory to extract the SM parameters or to look for yet-unknown particles and interactions but also help to pin-down the strong interaction dynamics at different scales from the Quantum Chormodynamics (QCD) point of view. It has been found that exclusive B-decays turn to be complicated as far as strong interactions required to study theoretically through the weak decays of b quark. Indeed, in the past few

decades, a reasonable number of literature has been devoted to understand the heavy-light mesons whose underlying weak decays are understandable but the complications appear during the study of strong interactions for their theoretical elucidation in the context of perturbative and non-perturbative QCD effects.

For their theoretical description, numerous techniques have been introduced to disentangle perturbative and non-perturbative affects of QCD that relies on the relatively large mass of the b-quark as compare to the strong interaction scale Λ_{QCD}. Actually, the mass of bottom quark m_b provides a scale at which the strong coupling α_s is smaller such that the short-distance effects are possible to calculate in perturbative manner. Aiming to deal with non-perturbative effects, various theoretical approaches are developed. Among them, the QCD factorization has emerged as the predominant theoretical framework which derives from the first principle [1].

The significant generation of weak gauge bosons at large hadron collider (LHC) is a source of inspiration to validate the predictions of the SM, search for the new physics (NP), improve our understanding about QCD dynamics at different regime and also offers opportunities to investigate exclusive hadronic decays. Among these decay modes, $W \to D_s\gamma$ stands out with the highest branching fraction. The first detailed analysis of radiative decay process $W \to D_s\gamma$ has been studied decades ago. The upper limit was set by CDF collaboration with the value $\mathcal{B}^{\text{Exp}}(W \to D_s\gamma) < 1.3 \times 10^{-3}$. This high-yield production of $W^{\pm}$ and Z has been a pivotal driver to unravel their decay characteristics with increased precision. In this context, several exclusive radiative decays of W and Z bosons into heavy-light meson have been investigated in the standard collinear factorization [2]. In this factorization, heavy-meson LCDAs appear in the formula are not completely non-perturbative, as they still entail the hard scale.

Nonetheless, the LCDA of heavy-light mesons defined the HQET framework is entirely nonperturbative which enters in HQET factorization formula. It is noteworthy to highlight that both types of LCDA associated with heavy-light meson are connected through perturbatively calculable matching coefficient [3]. The HQET factorization formula crucially depends on the mass hierarchy: $m_W \sim m_b \gg \Lambda_{\text{QCD}}$. This hierarchy ensures that the LCDA's dependence is confined to the soft scale, consequently, the LCDAs behavior is not entangled with perturbative effects. This separation of scales, facilitated by the mass hierarchy, allows for a more tractable and precise description of the heavy meson HQET LCDA. Notably, the production of heavy-light mesons within the HQET factorization formalism has been comprehensively addressed in [3] upto NLO in α_s, shedding light on the application of this factorization formula in the study of these processes. Furthermore, the exclusive production of flavoured quarkonia, such as $W^+ \to B_c^+\gamma$, has also been ivestigated through $\mathcal{O}(\alpha_s)$ within the NRQCD factorization framework [4].

In view of the kinematical scales involved in the study of hadrons, various types of theoretical approaches have been built up. QCD factorization is one of the crucial approach developed by Brodsky and Lepege [5]. it provides a theoretical basis to study

the QCD effects in exclusive processes.

This factorization helps to write the decay amplitude in term of short distance and long distance physics. QCD factorization simplifies the weak decays in heavy quark limit $m_b \gg \Lambda_{\text{QCD}}$ [6]. The heavy quark expansion allows for the study of several areas of B-physics, including inclusive rates and exclusive semi-leptonic decays. The physical idea of color transparency explains the relevance of the heavy-quark limit.

Soft QCD interactions decouple from a fast-moving light meson produced from a point-like source (a local operator in the effective weak Hamiltonian). More precisely, the couplings of soft gluons to such a system may be assessed by a multipole expansion, where a power of Λ_{QCD}/m_b suppresses the initial contribution (from the color dipole). Based on the heavy quark expansion, the QCD factorization technique offers the theoretical foundation for a systematic investigation of hadronic and radiative exclusive B decay amplitudes [6].

The factorization framework was initially employed in collider physics experiments like Deep Inelastic Scattering and hard hadron scattering experiments like the Drell-Yan process. The explanation of such processes is based on the parton model, which states that the partons that make up a hadron are mutually free. Such scatterings have total cross sections equal to a convolution integral of a hard perturbative parton-level cross-section with a process-independent, non-perturbative parton distribution function [7]. The weak decays amplitudes can be understood under the factorization framework. There are two types of forces involved in these process.

The HQET factorization formula for the decay process $W^+ \to B^+(D_s^+)\gamma$ has previously been established in [3] for the scenario where photon is energetic, $q^- \gg \Lambda_{\text{QCD}}$. In our study, we extends the decay of $W^+ \to B^+(D_s^+)\ell^+\ell^-$ where we have taken in account q^2 as non-zero (but small), and also q^2 is the invariant mass squared of the $\ell^+\ell^-$ pair originating from the virtual photon. Our primary objective is to perform a comprehensive calculation of the form factors associated with the $W^+ \to B^+(D_s^+)\ell^+\ell^-$ process within HQET framework, upto NLO in α_s.

3

2

Chapter 2

Factorization

Factorization is a method of separating the long-distance contributions in a process from the short-distance part, which is solely dependent on a large scale m_b. The computation of the short-distance part may be expressed as a series expansion in the strong coupling $\alpha_s(m_b)$. The long-distance contributions must be calculated using non-perturbative methods or established via experimental approaches. The benefit lies in the fact that these non-perturbative elements often exhibit a simpler structure compared to the original quantity, or they are not influenced by the specific process [1].

When considering the weak decays of heavy-light mesons, there are three primary kinematic scales. Specifically, the scales of interest are the masses of the weak boson m_W, the heavy quark m_b (in this instance, the b quark), and the scale of non-perturbative QCD interactions Λ_{QCD}. When examining this process at the heavy quark limit, these scales exhibit a hierarchical structure as follows:

$$m_W \gg m_b \gg \Lambda_{\mathrm{QCD}} \tag{2.1}$$

The weak interactions give rise to hadronic processes that can be described by the following form:

$$\mathcal{A}\left(\mathrm{B} \to \mathrm{M_1 M_2}\right) = \frac{\mathrm{G}_F}{\sqrt{2}} \sum_i \lambda_i \mathrm{C}_i(\mu) \left\langle \mathrm{M_1 M_2} \left| \mathcal{O}_i \right| \mathrm{B} \right\rangle (\mu) \tag{2.2}$$

The four fermion effective coupling is denoted as G_F, the CKM elements are represented by λ_i, and the short distance Wilson coefficients of the long distance effective operators $O_i(\mu)$ are denoted as C_i. The most challenging theoretical task is to calculate these elements of a matrix or, at the very least, to simplify them into more manageable non-perturbative entities. There are different approaches to simplify this difficulty [1].

2.1   Naive factorization

The first method, referred as "naive factorization", involves substituting the matrix element of a four-fermion operator in a heavy-quark decay with the product of the matrix elements of two currents [8]. An appropriate decay process to start the conversation would be

$$B \to \pi^+ \pi^-$$

under naive factorization we can write as

$$\left\langle \pi^+ \pi^- \left| (\bar{u}b)_{V-A} (\bar{d}u)_{V-A} \right| \bar{B}_d \right\rangle \to \left\langle \pi^- \left| (\bar{d}u)_{V-A} \right| 0 \right\rangle \left\langle \pi^+ \left| (\bar{u}b)_{V-A} \right| \bar{B}_d \right\rangle \tag{2.3}$$

By this way, the matrix element has been simplified into the product of decay constant and form factor of $\bar{B} \to \pi^+$. Due to gluon exchange, the π^- and $(\bar{B}\pi^+)$ system might interact, resulting in non-factorizable gluon contributions. This interaction can only be ignored if the virtual gluon is below the $\mu \sim m_b$.

2.2   QCD Factorization

The factorization of decay amplitude of heavy-light mesons into a convolution of hard kernel (T) and light cone distribution is possible due to the existence of widely separated kinematics scales. The B meson is considered the hydrogen atom in the field of quantum-chromodynamics (QCD), being the most basic non-trivial hadron. In the leading approximation, the b quark remains stationary at the origin and generates a chromo-electric field. Light degrees of freedom like gluons and light quarks moves in external fields [9].

The usual mass and energy scales used in the creation of B mesons are $m_b = 4.8$ GeV, $m_W = 80$ GeV, and the momentum scale of the non-perturbative QCD interaction $\Lambda_{\text{QCD}} = 0.2$ GeV. The two-meson final state determines the factorization characteristics of non-leptonic decay amplitudes. A meson is considered "light" if, at the heavy-quark limit, its mass m does not become infinite. If we suppose that the mass scale of a meson within m_b in heavy-quark limit, i.e., m/m_b remains constant, then we conclude that meson is heavy. For a light meson, it is still possible to have $m \gg \Lambda_{\text{QCD}}$.

In the heavy-quark limit, we examine weak decays $B \to M_1 M_2$ and segregate decays into final states that include either one heavy meson and one light meson or two light mesons [1]. The factorization formula takes the following form in the case of both mesons M_1 and M_2 are light mesons

$$\left\langle M_1 M_2 \left| \mathcal{O}_i \right| \bar{B} \right\rangle = \sum_j F_j^{B \to M_1} \left(m_2^2 \right) \int_0^1 du\, T_{ij}^I(u) \Phi_{M_2}(u) + (M_1 \leftrightarrow M_2)$$

$$+ \int_0^1 d\xi du dv\, T_i^{II}(\xi, u, v) \Phi_B(\xi) \Phi_{M_1}(v) \Phi_{M_2}(u) \tag{2.4}$$

5

Lets suppose M_1 is heavy and M_2 is light meson, in this case the factorization formula takes the form [1]

$$\langle M_1 M_2 \left| \mathcal{O}_i \right| \bar{B} \rangle = \sum_j F_j^{B \to M_1} \left(m_2^2 \right) \int_0^1 du T_{ij}^I(u) \Phi_{M_2}(u) \tag{2.5}$$

The factorization formula graphical representation can be illustrated as
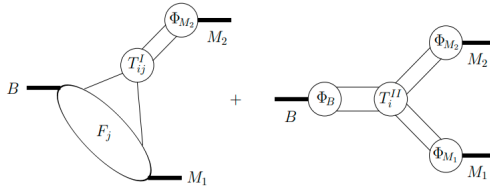
Figure 2.1: Factorization formula graphical representation

$F_j^{B \to M_{1,2}}(\mathrm{m}_{2,1}^2)$ is a B → $M_{1,2}$ form factor, $\Phi_X(\mathrm{u})$ is the light-cone distribution amplitude for the quark-antiquark fock state of X meson. $T_j^I(u)$ and $T_j^{II}(\xi, u, w)$ are hard-scattering kernels, which are calculated perturbatively. The hard-scattering kernels and LCDAs are factorization scale dependant. Finally, $m_{1,2}$ denote the light meson masses [1].

2.3   Non-Perturbative Quantities

Non perturbative region is the region where strong forces dominate and coupling is strong enough to make the bound states. Due to strong coupling constant, we can no longer expand the theory perturbativily in term of coupling constant.

2.3.1   Form Factors

The weak hadronic current's matrix elements include certain scalar functions of the four-momentum transfer squared, q^2, referred to as form factors. These previously unidentified functions are intended to include all information on the modifications of the fundamental weak interaction caused by "virtual" strong interactions. Likewise, the matrix components of meson decays may be represented using established kinematic quantities and first unidentified form factors that characterize the "virtual" effects of strong interactions. To get a full understanding of weak processes, it is essential to possess understanding of the associated form factors. This entails the ability to

compute the strong interaction effects that these form factors represent [10].

Form factors are made up of independent components that are produced by applying gauge symmetry and Lorentz decomposition to current matrix elements. Two scalar form factors are used in QCD factorization to parameterize the vector currents' matrix elements: $F_+^{B \to P}\left(q^2\right)$ and $F_0^{B \to P}\left(q^2\right)$. The vector matrix element B to pseudo-scalar (P) is parameterized as

$$\left\langle \mathrm{P(k)}\left|\bar{\mathrm{q}}\gamma^\mu \mathrm{b}\right| \bar{\mathrm{B}}(p)\right\rangle = \mathrm{F}_+^{\mathrm{B} \to P}\left(p^\mu + k^\mu\right) + \left[F_0^{B \to P} - F_+^{B \to P}\right]\frac{m_B^2 - m_P^2}{q^2}q^\mu \qquad (2.6)$$

Here, q represents the difference in momentum among the two mesons. The two form factors become about equal as the difference in momentum among the final and first mesons approaches zero. The previously mentioned form factors are referred to as physical form factors. Using these form factor are beneficial since they are connected to measurable quantities or with other form factors derived from LQCDs or QCD sum rules.

2.3.2 Light Mesons LCDA's

The momentum distribution for light mesons is determined by their corresponding Light-Cone Distribution Amplitudes (LCDA's) in exclusive processes. This is comparable to Parton distribution functions for inclusive processes. Typically, they refer to matrix components of a two-quark bi-local operator between vacuum and meson states. The primary twist light-cone distribution amplitudes (LCDA's) for Pseudo-scalar (P), longitudinally polarized Vector ($V_{||}$), and transversely polarized Vector ($V_\perp$) mesons are shown below, inside the heavy quark limit.

$$\left\langle \mathrm{P(q)}\left|\bar{\mathrm{q}}(y)_\alpha \mathrm{q}'(x)_\beta\right|0\right\rangle\bigg|_{(x-y)^2=0} = \frac{i\mathrm{f}_P}{4}\left(\not{q}\gamma_5\right)_{\beta\alpha}\int_0^1 du e^{i(\bar{u}qx + uqy)}\Phi_P(u,\mu),$$

$$\left\langle \mathrm{V}_{||}(q)\left|\bar{q}(y)_\alpha \mathrm{q}'(x)_\beta\right|0\right\rangle\bigg|_{(x-y)^2=0} = -\frac{i\mathrm{f}_V}{4}\not{q}_{\beta\alpha}\int_0^1 du e^{i(\bar{u}\mathrm{q}x + uqy)}\Phi_{||}(u,\mu), \qquad (2.7)$$

$$\left\langle \mathrm{V}_\perp(q)\left|\bar{q}(y)_\alpha \mathrm{q}'(x)_\beta\right|0\right\rangle\bigg|_{(x-y)^2=0} = -\frac{i\mathrm{f}_T(\mu)}{8}\left[\not{\epsilon}_\perp^*, \not{q}\right]_{\beta\alpha}\int_0^1 du e^{i(\bar{u}qx + uqy)}\Phi_\perp(u,\mu)$$

The form factors of their respective mesons are denoted as $f_{P, V_{||}, V_\perp}(\mu)$ representing the mesons.

2.3.3 B-Mesons LCDA defined in QCD

Since LCDAs are defined using light-cone coordinates, detailed descriptions of these coordinates are provided in Chapter 4 with thorough explanations. The motivation for

the inclusion of the B meson Light-Cone Distribution Amplitude (LCDA) in the QCD factorization framework is the hard interaction of spectator quark. The hard spectator interaction term is determined by the dot product of p' and l, where p' represents the momentum of the light meson and l represents the momentum of the spectator quark. Since only the p'_- component of the light meson momentum is non-zero, the dot product $p' \cdot l$ may be simplified to $p'_- l_+$. The decay amplitude of the two-particle Fock state of the B meson is given by:

$$\Psi_{B(z,p)} = \left\langle 0 \left| \bar{q}_\alpha(z)[z,0]b_\beta(0) \right| \bar{B}_d(p) \right\rangle = \int \frac{d^4 l}{(2\pi)^4} e^{-ilz} \hat{\Psi}_B(l,p) \tag{2.8}$$

The symbol $\hat{\Psi}_B$ denotes the complete Bethe-Salpeter wave function, whereas [z, 0] symbolizes the Wilson line, which guarantees the bi-local gauge invariance of the matrix element. Subsequently, estimating the result as

$$\int \frac{d^4 l}{(2\pi)^4} A(l,\dots) \hat{\Psi}_B(l,p) = \int dl^+ A\left(l^+,\dots\right) \int \frac{d^2 l_\perp \} textdl^-}{(2\pi)^4} \hat{\Psi}_B(l,p) \tag{2.9}$$

At leading order B meson LCDA can be expressed using two scalar wave functions:

$$\left\langle 0 \left| \bar{q}_\alpha(z)[z,0]b_\beta(0) \right| \bar{B}_d(p) \right\rangle = -\frac{if_B}{4} \delta_{ij} \left[(\not{p} + m_b) \gamma_5 \right]_{\beta\gamma}$$
$$\times \int_0^1 d\xi e^{-i\xi p^+ z^-} \left[\Phi_{B1}(\xi) + \not{n}^- \Phi_{B2}(\xi) \right]_{\gamma\alpha} \tag{2.10}$$

The re-normalization conditions are

$$\int_0^1 d\xi \Phi_{B1}(\xi) = 1, \quad \int_0^1 d\xi \Phi_{B2}(\xi) = 0 \tag{2.11}$$

where $\xi \equiv l_+/p_+$ is the s longitudinal momentum fraction of spectator quark. one can neglect the difference of B-meson and b-quark at the leading order in $\mathcal{O}(1/m_b)$

Chapter 3

Heavy Quark Effective Theory

In this chapter, we will discuss heavy quark effective field theory and motivation behind it. We will derive Feynman rules of HQET to solve the heavy quark b wave function correction. LCDA's of B Meson will also be defined in HQET.

There are total six quarks in SM. Three of them are heavy quarks named as top t, bottom b and charm c quarks. Their masses are very large then the Λ_{QCD} scale where quarks are in bound state. Top quark physics can accurately be predicted perturbivily since $m_{top} >> \Lambda_{\text{QCD}}$. For bound state of other two quarks b and c we can use the heavy quark limit, by expanding the Λ_{QCD}/m_b and Λ_{QCD}/m_c respectively. For light quarks mesons, $m_q < \Lambda_{\text{QCD}}$ and so we can use the limit $m_q = 0$. Under this limit, QCD Lagrangian is reduced to low energy chiral Lagrangian where m_q is the mass of light quark.

3.1 Physical picture of HQET

In heavy quark limit, the heavy light mesons are very similar to the hydrogen atom. To proceed the discussion, we will discuss B-meson. Just like in hydrogen atom, proton is static and electron is revolving around it under the Coulomb potential which is provided by the proton. In B-meson, the b-quark behaves like the proton and is at rest and anti-up quark is very light as compare to the b, so it does behave like electron. But as the QCD is strongly coupled at low energies, we cannot directly relate the Coulomb potential to the Strong force potential. QCD can represent the interactions between gluons and all types of quarks, but for heavy-light mesons, HQET is a more appropriate approximation. This works due to the substantial disparity in mass between one of the constituent quarks and the other quark, as well as the interchange of momentum that keeps the meson bound together. The effective theory is obtained by taking the limit of heavy quark mass in QCD, $m_Q \to \infty$, resulting in the emergence of fascinating symmetries like heavy quark spin symmetry [11].

The spin of B-meson ($b\bar{u}$) is $\frac{1}{2} \otimes \frac{1}{2} = 0 \oplus 1$. The leading order spin state-0 is of B-meson and NLO spin state-1 triplet state is of B^* which is the excited state of B-meson. The mass difference in these two states is analogous to the energy states difference between the S (spin singlet) and P(spin triplet) states of hydrogen atom in fine structure. Experimentally determined mass difference between these two states are 44MeV. At leading order Λ_{QCD}/m_b, the B-meson is is independent of spin and both B and B^* are in degenerate state. This is known as Heavy quark-spin symmetry [7] Other then spin symmetry, there is another important symmetry called Heavy quark-flavor symmetry where we take the limit $m_Q \to \infty$. At this limit the heavy quark is stationary and acts as the stationary source of gluons. At leading order $1/m_Q$, the dynamics is independent of the flavour of the quark and it puts very important constrain on heavy hadron physics [11].

3.2   Heavy quark symmetry

For a number of reasons, the strong interactions in systems with heavy quarks are easier to understand than one with light quarks only. Asymptotic freedom, or the weakening of QCD's effective coupling constant in processes involving substantial momentum transfer, which corresponds to interactions at small distance scales, is one crucial feature.

$$\alpha_s\left(Q^2\right) = \frac{g_{\text{eff}}^2\left(Q^2\right)}{4\pi} = \frac{12\pi}{\left(33 - 2n_f\right)\ln(Q^2/\Lambda_{\text{QCD}}^2)} \tag{3.1}$$

The effective coupling constant exhibits a drop as the value of Q^2 increases, resulting in a weakening of strong interactions at shorter distances. At large distances (with a small Q^2), the coupling becomes strong, results in nonperturbative effects like confinement of quarks and gluons on a long scale $R_{\text{had}} \sim 1/\Lambda_{\text{QCD}} \sim 1\text{fm}$. For heavy quark he effective coupling constant $\alpha_s(m_Q)$ is quite small. The scale is comparable to the Compton wavelength $\lambda_Q \sim 1/m_Q$.
The complexity of systems consisting of a heavy quark and other light components is heightened. The overall size of these systems are dictated by R_{Had}, and the typical momenta transferred between the heavy and light elements are of order Λ_{QCD}.

$$m_Q\Lambda_{\text{QCD}} \to \lambda_Q \ll R_{had} \tag{3.2}$$

To determine the quantum numbers of the heavy quark, a rigorous investigation using a $Q^2 \geq m_Q^2$ would be necessary. The gluons that form soft couplings with the "brown muck" are limited to resolving distances much greater than λ_Q. Hence, the degrees of freedom associated with light are independent of the flavor(mass) and spin orientation of the heavy quark. They just see the colour force, which spans large distances because to confinement. In the rest frame of the heavy quark, the electric colour field is

10

the only significant factor, whereas relativistic phenomena such as colour magnetism diminish as the $m_Q \to \infty$ increases. The decoupling of the heavy quark spin occurs due to its exclusive involvement in interactions mediated by relativistic processes. The insignificance of the heavy quark mass may be seen in the following manner: Therefore, at the $m_Q \to \infty$ limit, hadronic systems that vary just in the flavour or spin quantum numbers of the heavy quark possess identical light degrees of freedom configurations.

3.3   HQR Mechanism

The primary goal of HQR is to give an accurate picture in the heavy quark limit for generation of hadrons with heavy flavors. This entails distinguishing between the effects of hadrons at $\mathcal{O}(\Lambda_{\mathrm{QCD}})$ and the dynamics of order m_b or higher. However, HQR no longer differentiates between the hard-scattering scale that is peculiar to the process, such as Q and m_b.

The basic idea underlying this process is extremely simple: in a hard scattering, there is a significant chance that the heavy quark will combine with a spectator quark. This process is relatively soft at rest, creating a heavy-light hadron. The HQR formalism alone includes a single nonperturbative component. In this context of the color-singlet channel, where the difference between inclusive and exclusive generation of heavy hadrons is minimal at the lowest order. According to HQET, this factor is exactly proportional to the B meson LCDA's first inverse moment [3].

The parton recombination model created by Das and Hwa in 1977 is where the word "recombination" in high energy physics first appeared. The purpose of this model was to describe how mesons are produced in hadronic collisions at low p'. In this case, the momentum of a valence particle in one of the colliding hadrons provides the bulk of the momentum of the meson. Recombination of a sea parton obtained from the same hadron with a valence parton yields the meson. Similar processes result in the production of heavy mesons by recombination, where a valence parton can impart a large amount of its momentum to the heavy meson. However, in this particular scenario, the valence parton interacts with a heavy quark generated during the process of hard scattering [12].

3.4   HQET Lagrangian

Consider an effective field theory where heavy symmetries is exact. Consider the momentum of B-meson is p^μ which can be decompose as

$$p^\mu = m_Q v^\mu + k^\mu \tag{3.3}$$

where v^μ is 4-velocity and $v^2 = 1$. k^μ is the momentum of all other soft degrees in B-meson and $k^\mu \sim \Lambda_{\mathrm{QCD}}$. If we consider to shift $k^\mu \to k^\mu + \Delta k^\mu$, and 4-velocity changes

as $v^\mu \to v^\mu - \Delta k^\mu/m_Q$ then at leading order $1/m_Q$, the interactions can only change v^μ by the factor of Λ_{QCD}/m_Q. So the velocity is unique at leading order and becomes quantum number for heavy quark effective field theory [7].

The QCD Lagrangian is given as

$$\mathcal{L}_{\text{QCD}} = \bar{\Psi}(i\slashed{D} - m_Q)\Psi \tag{3.4}$$

where $\slashed{D}$ is covariant derivative and m_Q is the mass of heavy quark. The QCD field $\Psi = e^{-im_Q v \cdot x}(\psi_v + \chi_v)$ where ψ_v is particle spinor and χ_v is anti-particle spinor. $e^{-im_Q v \cdot x}$ filters out the hard degrees of freedom from soft degrees of freedom in bound state. Dirac equation for heavy quark can be written as

$$(m_Q\slashed{v} + k)\Psi = m_Q\Psi \tag{3.5}$$

We can expand it in term of mass as

$$\left(1 - \slashed{v} - k/m_Q\right)\Psi = 0 \tag{3.6}$$

To satisfy the Eq 3.4, both spinors have to satisfy the following equations

$$\left(\frac{1 + \slashed{v} + \frac{k}{m_Q}}{2}\right)\Psi = \psi_v \quad \text{and} \quad \left(\frac{1 - \slashed{v} - \frac{k}{m_Q}}{2}\right)\Psi = \chi_v \tag{3.7}$$

Term k/m_Q is suppressed due to heavy quark mass limit $m_Q \to \infty$. The term $1 \pm \slashed{v}$ acts like a projection operators to project out the particle and anti particle spinors when acts on heavy quark field Ψ. From Dirac field we can conclude that

$$\psi_v \approx \left(\frac{1 + \slashed{v}}{2}\right)\Psi \quad \text{and} \quad \chi_v \approx 0 \tag{3.8}$$

This shows that pair production is not allowed in HQET as anti-particle spinor is suppressed. So we can write the heavy quark field as $\Psi = e^{-im_Q v \cdot x}\psi_v$ and QCD Lagrangian can be expressed as

$$\mathcal{L}_{\text{HQET}} = e^{im_Q v \cdot x}\bar{\psi}_v(i\slashed{D} - M)e^{-im_Q v \cdot x}\psi_v \tag{3.9}$$

Covariant derivative $\slashed{D}$ is given as

$$\slashed{D} = \slashed{v}v \cdot D + \slashed{D}_\perp \tag{3.10}$$

$$\mathcal{L}_{\text{HQET}} = e^{im_Q v \cdot x}\bar{\psi}_v\left(i\gamma^\mu(\partial_\mu + igA_\mu) + i\slashed{D}_\perp - m_Q\right)e^{-im_Q v \cdot x}\psi_v \tag{3.11}$$

$$\mathcal{L}_{\text{HQET}} = \bar{\psi}_v\left(-(1 - \slashed{v})m_Q + iv \cdot (\partial + igA)\right)\psi_v \tag{3.12}$$

12

and we have shown above that anti-spinor is suppressed so $(\not{v} - 1)\psi_v = 0$. At leading order in m_Q, the effective Lagrangian takes the following form [13, 11]

$$\mathcal{L}_{\text{HQET}} = \bar{\psi}_v(iv \cdot D)\psi_v + \mathcal{O}\left(1/m_Q\right) \tag{3.13}$$

There is no mass of heavy quark involved in Lagrangian which is due to the heavy quark flavour symmetry. Under this symmetry, there is no way to distinguish between the different heavy quarks flavours as we have discussed above. There is no gamma matrices involved in HQET Lagrangian showing that its SU(2) Lagrangian [13, 11].

3.5   Feynman rules of HQET

The HQET Lagrangian can be written explicitly as

$$\mathcal{L}_{\text{HQET}} = i\bar{\psi}_v v \cdot \partial\psi_v + ig\bar{\psi}_v v \cdot A\psi_v \tag{3.14}$$

One can get the Feynman rules from this lagrangian as heavy quark propagator gives $\frac{1}{v.p}\delta_{ij}$ and heavy quark- gluon vertex gives $-igT^a v^\mu$. We can directly calculate these Feynman rules as from simple Feynman propagator. The Feynman propagator is given as

$$\frac{\not{p} + m_Q}{p^2 - m_Q^2}\delta_{ij} \tag{3.15}$$

where

$$p^\mu = m_Q v^\mu + k^\mu \tag{3.16}$$

So the Eq 3.15 becomes

$$=\frac{\not{v} + 1 + \frac{k}{m_Q}}{2v \cdot k + \frac{k^2}{m_Q}}\delta_{ij} \tag{3.17}$$

and we get our propagator with the projection operator

$$= \frac{\not{v} + 1}{2v \cdot k}\delta_{ij} + \mathcal{O}\left(k/m_Q\right) \tag{3.18}$$

For quark gluon vertex, consider QCD vertex as $ig\gamma^\mu T^a$. We can write it in HQET as follow

$$= \frac{1 + \not{v}}{2}\gamma^\mu\frac{1 + \not{v}}{2} \tag{3.19}$$

and we can simplify it as

$$= -igT^a v^\mu \tag{3.20}$$

13

3.6 Heavy Quark Self Energy Diagram

Consider the following self energy diagram
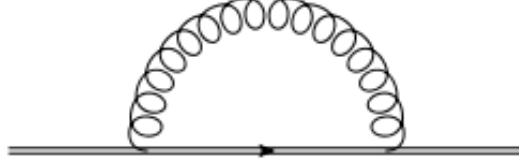
Figure 3.1: Heavy quark self energy diagram with outgoing loop momentum l

By using the derived Feynman rules in section 3.5 we can write amplitude of above diagram as following

$$\Sigma_Q = -C_F g^2 \mu^{2\epsilon} \int \frac{d^D l}{l^2} \frac{v^2}{[v \cdot (p - l)]} \tag{3.21}$$

by using Feynman parametrisation technique to simplify the denominator

$$\frac{1}{AB} = \int_0^\infty dy \frac{1}{(A + yB)^2} \tag{3.22}$$

With the help of this formula, we can write the amplitude in this way considering $v^2 = 1$.

$$\Sigma_Q = -C_F g^2 \mu^{2\epsilon} \int_0^\infty dx \int d^D l \frac{1}{(l^2 + xv \cdot (p - l))^2} \tag{3.23}$$

We can integrate the loop momenta by using [14]

$$\int d^D l \frac{1}{[l^2 + 2l \cdot Q - R^2]^n} = \frac{(-1)^n i \pi^{D/2} \Gamma(n - D/2)}{\Gamma(n)[Q^2 + R^2]^{n - D/2}} \tag{3.24}$$

where $D = 4 - 2\epsilon$, l is our loop momentum, $Q^2 = \frac{v^2}{4}$ and $R^2 = -yv.p$. This simple propagator reduced to the following result by using Eq 3.24

$$\Sigma_Q = i\pi^{\frac{3}{2} - \epsilon} \mu^{2\epsilon} \Gamma(1 - \epsilon) \Gamma\left(\epsilon - \frac{1}{2}\right) \Gamma(\epsilon) \left(-\frac{1}{p.v}\right)^\epsilon (-p.v)^{1 - \epsilon} \tag{3.25}$$

14

by expanding this result in the power of ϵ we can write it out as

$$\Sigma_Q = 2p.v \left(\frac{1}{\epsilon} + 2\log(\mu) + \log\left(-\frac{1}{p.v}\right) - \log(-4\pi p.v) + 2 \right) \qquad (3.26)$$

The first term $\frac{1}{\epsilon}$ is UV divergence and will be cancelled out by adding the counter term diagram so we are left with the heavy quark self energy diagram result as

$$\Sigma_Q = 2p.v \left(2\log(\mu) + \log\left(-\frac{1}{p.v}\right) - \log(-4\pi p.v) + 2 \right) \qquad (3.27)$$

3.7 Re-normalization of HQET Propagator

Bare heavy quark field contains the counter term

$$\psi_0 = \left(1 + \frac{\delta_\psi}{2} \right) \psi \qquad (3.28)$$

The bare propagator is given as [15]

$$G_0 = Z_\psi G \qquad (3.29)$$

where Z is the counter term. Consider the following 1IP loop diagram
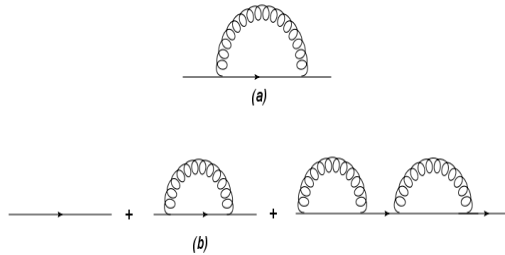

Figure 3.2: (a) Self energy of single heavy quark. (b) Calculating the total heavy quark propagators by considering both the tree level and up to N 1PI self energy loop corrections.

15

By taking the sum of the increasing number of loops as shown in Fig 3.2 (b)

$$iG_0 = \frac{i(1+\not v)}{v \cdot k} + \frac{i(1+\not v)}{v \cdot k} \sum_Q + \frac{i(1+\psi)}{v \cdot k} + \dots \tag{3.30}$$

We can express this sum up this series as geometric series and we get the following result

$$iG_0 = \frac{i(1+\not v)}{v \cdot k} \left[\frac{1}{1 + \frac{(1+\not v)\sum_Q}{v \cdot k}} \right] \tag{3.31}$$

So we can express the re- normalized propagator as

$$iG^R = \frac{1}{1+\delta_\psi} \frac{i(1+\not v)}{v \cdot k + (1+\not v) \sum_Q} \tag{3.32}$$

By expanding only in first order of ϵ, we can write the re-normalized propagator as

$$iG^R = \frac{i(1+\not v)}{v \cdot k + (1+\not v) \sum_Q + \delta_\psi v \cdot k + \mathcal{O}\left(\frac{1}{\epsilon^2}\right)} \tag{3.33}$$

Only divergence of order $\frac{1}{\epsilon}$ has been retained in counter term.

3.8   HQET Factorization for Radiative B Decay

In order to concentrate on the fundamental aspects of the topic, we will confine our attention to a more straightforward process $\mathcal{B} \to \gamma l \bar{\nu}_l$ outlined in [16]. The factorization of the given process involves just the hard photon and weak boson as the final states. The factorization of this is carried out at the tree level and includes QCD corrections up to the first order gluon loop. As a result of the lack of mesons i n the final state, the HQET factorization formula for this simply comprises the second convolution integral.

$$\mathcal{M} = \int_0^\infty d\omega \, T^{II}(\omega, \mu_F)\Phi(\omega, \mu_F) + \mathcal{O}(1/m_b) \tag{3.34}$$

where ω represents the momentum of the light quark, whereas μ_F denotes the factorization scale that distinguishes between the long and short distance physics. Therefore, it may be represented as a expression that is organized by order by order.

$$\mathcal{M}^{(0)} + \mathcal{M}^{(1)} + \dots = \Phi^{(0)} \otimes T^{(0)} + \Phi^{(1)} \otimes T^{(0)} + \Phi^{(0)} \otimes T^{(1)} + \dots \tag{3.35}$$

It can be shown that factorisation is valid up to one loop order and does not need reliance on any transverse components.

3.8.1   Light Cone Distribution Amplitudes (LCDAs) in HQET

When in hard exclusive QCD processes the internal composition of hadrons when examined is known as light-cone distribution amplitudes (LCDAs). These factors are non-perturbative and play a crucial role in the theory and in the study of strong interactions. LCDAs of heavy hadrons are used in many computations, such as the generation of heavy hadron pairs, as well as in the examination of symmetry relationships between the form factors that describe the transitions between heavy and light mesons [17] .

B-meson light cone distribution amplitude (LCDA) is an essential nonperturbative factor that consistently appears in different exclusive B decay processes. The entity that enters the B exclusive production process in the HQET factorization framework is identical. Let's examine the co-relator consisting of the light spectator quark and b-quark. They are separated at a light-like distance, enclosed in a vacuum with B meson moving with velocity of v. The most general way to express it is in the following manner[3]

$$\left\langle B(v)\left|\bar{u}_\beta(z)[z,0]h_{v,\alpha}(0)\right|0\right\rangle = \frac{i\hat{f}_B m_B}{4}\left\{\left[2\widetilde{\phi}_B^+(t) - \frac{\not{z}}{t}\left(\widetilde{\phi}_B^-(t) - \widetilde{\phi}_B^+(t)\right)\right]\frac{1-\not{v}}{2}\gamma_5\right\}_{\alpha\beta}$$

where $z^2 = 0$, the product of v and z the is defined as variable t, and ϕ_B^+ represents a pair of nonperturbative functions that depend on t. u represents the standard QCD field for the u quark. h_v denotes the b quark field with the velocity label v introduced in HQET. α and β represent spinor indices. f_B represents the decay constant of the B meson, which is specified in HQET as following [3]

$$\langle B(v)|\bar{u}\gamma^\mu\gamma_5 h_v|0\rangle = i\hat{f}_B m_B v^\mu \tag{3.36}$$

B-meson decay factor $\hat{f}_B$ upto one loop is given as [3]

$$\hat{f}_B(\mu_F) = \left[1 + \frac{\alpha_s C_F}{4\pi}\left(3\ln\frac{\mu_F}{m_b} + 2\right)\right]f_B \tag{3.37}$$

The term [z, 0] denotes the Wilson line, which is used to guarantee bi-local gauge invariance of the matrix element.

$$[z,0] = \mathcal{P}\exp\left[-ig_s\int_0^z d\xi^\mu A_\mu^a(\xi)t^a\right] \tag{3.38}$$

The expression t^a $(a = 1,\ldots,8)$ represents the generators of SU(3) in the basic representation, while $\mathcal{P}$ denotes the path ordering.

When the hard-scattering kernel T is computed using fixed-order perturbation theory,

only the logarithmic moments of the light-cone distribution amplitude (LCDA) are examined. In momentum space, B meson LCDA can be expressed as

$$\Phi_B^\pm(\omega) \equiv i\hat{f}_B m_B \phi_B^\pm(\omega) = \frac{1}{v^\pm} \int \frac{dt}{2\pi} e^{i\omega t} \left\langle B(v) \left| \bar{u}(z)[z,0]\slashed{n}_\mp \gamma_5 h_v(0) \right| 0 \right\rangle \Bigg|_{z^+, z^\perp = 0} \tag{3.39}$$

where the pair of B-meson LCDAs are defined as

$$\phi_B^\pm(\omega) = \int_0^\infty \frac{dt}{2\pi} e^{i\omega t} \widetilde{\phi}_B^\pm(t) \tag{3.40}$$

Both quantities $\Phi_B^\pm(\omega)$ are scale dependant and are evolved by Lange-Neubert equation [18]

$$\frac{d}{d\ln\mu}\phi_B^+(\omega,\mu) = -\frac{\alpha_s C_F}{4\pi} \int_0^\infty d\omega' \left\{ \left(4\ln\frac{\mu}{\omega} - 2\right) \delta\left(\omega - \omega'\right) - 4\omega \left[\frac{\theta\left(\omega' - \omega\right)}{\omega'\left(\omega' - \omega\right)} \right. \right.$$
$$\left. \left. + \frac{\theta\left(\omega - \omega'\right)}{\omega\left(\omega - \omega'\right)} \right]_+ \right\} \phi_B^+\left(\omega',\mu\right) \tag{3.41}$$

Where μ is the our normalization scale and it usually ranges $1\text{GeV} \leq \mu \leq m_b$.

3.8.2 Momentum Space Projector of B Meson

Consider Eq 3.36, If we choose the pre factors such that z = 0 and $\widetilde{\phi}_B^+(t) = \widetilde{\phi}_B^-(t) = 0$ By using identity given as

$$\int d^4 z\, M(z)T(z) = \int \frac{d^4 k}{(2\pi)^4}\, T(k) \int d^4 z\, e^{-ikz} M(z) = \int_0^\infty dk^+\, M^B T(k) \Bigg|_{k=kn^-} \tag{3.42}$$

here $M(z)$ is the position space projector and $T(z)$ is hard scattering kernel in position space. In order to get the position space operator for the B meson from Eq 3.42, we first break down the momentum k into light cone components.

$$\int d^4 z M(z)T(z) = \frac{i\hat{f}_B m_B}{4} \left\{ \left(\frac{1-\slashed{v}}{2}\right) \int_0^\infty d\omega \left[2\phi_B^+(\omega) + \right. \right.$$
$$\left. \left. \int_0^\omega d\eta \left(\phi_B^-(\eta)\phi_B^+(\eta)\right) \gamma^\mu \frac{\partial}{\partial k_\nu} \right] \gamma^5 \right\}_{\alpha\beta} T_{\alpha\beta}(k) \Bigg|_{k=\omega v}$$

We can write the Hard scattering kernel amplitude in heavy quark limit as

$$T(k) = T^{(0)}(k^+) + k_\perp T_\mu^{(1)}(k^+) \tag{3.43}$$

18

By decomposing partial derivative $\frac{\partial}{\partial k}$ into light cone we can get the B-meson space projector from **??**

$$
\mathcal{M}_B^{\alpha\beta} = \frac{i\hat{f}_B m_B}{4} \left\{ \frac{1 - \not{v}}{2} \left[\Phi_B^+(\omega)\not{n}^+ + \Phi_B^-(\omega)\not{n}^- \right. \right.
$$
$$
\left. \left. - \int_0^\omega d\eta \left(\Phi_B^-(\eta) - \Phi_B^+(\eta) \right) \gamma^\mu \frac{\partial}{\partial k_\perp^\nu} \right] \gamma^5 \right\}_{\alpha\beta} \tag{3.44}
$$

3.8.3 Phenomenological Parameters of B Meson

We can write the form factors in term of some unique integrals which are known as inverse moments. The first inverse moment is given as [3]

$$
\lambda_B^{-1}(\mu) \equiv \int_0^\infty \frac{d\omega}{\omega} \phi_B^+(\omega, \mu) \tag{3.45}
$$

and logarithmic inverse movements are given as

$$
\lambda_B^{-1}\sigma_{B,n}(\mu) \equiv -\int_0^\infty \frac{d\omega}{\omega} \ln^n \frac{\omega}{\mu} \phi_B^+(\omega, \mu) \tag{3.46}
$$

We have used till 2nd logarithmic moment. ϕ_+ depends on scale μ_F, which is factorization scale typically ranges from 1GeV to m_b. The evolution of Φ_+ is given by Lange-Neubert equation.

Chapter 4

Factorization of the Amplitude $W^+ \to B^+\gamma$

To calculate the vector and axial vector form factors which appear in amplitude while writing it under given symmetries of theory, we calculate the Feynman amplitude at LO and NLO and then calculate LCDAs. By writing the Feynman amplitude in the form of convolution, we calculate the hard scattering kernel at LO and NLO. After calculating both LCDAs and hard kernel at LO and NLO, we calculate both form factors.

In this chapter, the radiative production of heavy light meson B is studied in the following decay

$$W^+ \to B^+\gamma$$

We calculate the Feynman amplitude in full QCD and LCDAs are calculated either in HQET or in QCD at LO and NLO. We write the full amplitude in term of convolution of hard scattering kernel and LCDAs. One loop gives rise six topological diagrams and every diagram corresponds to its own LCDAs and hard kernel. Final hard scattering kernel is the sum of all six hard kernels.

The hadronic matrix element can be written in term of factors as

$$\mathcal{M}\left(W^+ \to B^+\gamma\right) = \frac{e_u e^2 V_{ub}}{4\sqrt{2}\sin\theta_W}\left(\epsilon_{\mu\nu\alpha\beta}\frac{P^\mu q^\nu \varepsilon_W^\alpha \varepsilon_\gamma^{*\beta}}{P \cdot q}F_V + i\varepsilon_W \cdot \varepsilon_\gamma^* F_A\right) \tag{4.1}$$

4.1 Kinematics of process

We can define the kimatics of this process in both frame of references, In B-meson rest frame or in W boson rest frame. For the sake of simplicity, we work in mass dimensions. W boson decays into B meson and hard photon. To conserve the momentum, both B meson and photon are in opposite direction to make the final momentum zero.

4.1.1 In W boson rest frame

Consider the W boson is in rest frame, decaying into the B meson moving in positive x axis of light cone coordinates and photon is moving in opposite direction for the conservation of momentum.

Four momenta of particles in W rest frame is given as follow

$$K^\mu = (m_W, \vec{0})$$
$$P^\mu = (E_B, \vec{p})$$
$$q^\mu = (E_\gamma, \vec{q})$$

We can write at due to conservation of momentum

$$K^\mu = P^\mu + q^\mu$$

and as we are working in W rest frame

$$K^\mu = (m_W, \vec{0})$$

which allows to write the four momenta as

$$P_B^\mu = \left(\frac{m_W^2 + m_B^2}{2m_W}, 0, 0, \frac{m_W^2 - m_B^2}{2m_W} \right)$$

$$q^\mu = \left(\frac{m_W^2 - m_B^2}{2m_W}, 0, 0, \frac{m_B^2 - m_W^2}{2m_W} \right)$$

The light cone representation of a vector is given as

$$n^\mu = \frac{1}{\sqrt{2}}(1, 0, 0, 1)$$

and

$$\bar{n}^\mu = \frac{1}{\sqrt{2}}(1, 0, 0, -1)$$

A vector in light cone basis can be given as

$$V^\mu = (V \cdot n)\bar{n}^\mu + (V \cdot \bar{n})n^\mu + V_\perp^\mu = V_+^\mu + V_-^\mu + V_\perp^\mu \tag{4.2}$$

In these basis, the momenta defined above can be expressed as following

$$K^\mu = \frac{1}{\sqrt{2}}(m_W, m_W, 0)$$

$$P_B^\mu = \frac{1}{\sqrt{2}} \left(m_W, \frac{m_B^2}{m_W}, 0 \right)$$

$$q^\mu = \frac{1}{\sqrt{2}} \left(0, m_W - \frac{m_B^2}{m_W}, 0 \right)$$

21

4.1.2 In the rest frame of B meson

HQET is defined in B meson rest frame, So we can consider B meson in rest and W boson and photon are moving in opposite direction. The photon is boosted along $-z$ axis. The photon momentum is B rest frame is invariant given as

$$q^\mu = (E_\gamma, 0, 0, -\vec{q}_z) \tag{4.3}$$

and

$$P^\mu = (m_B, 0, 0, 0) \tag{4.4}$$

$$q^\mu = \left(\frac{m_W^2 - m_B^2}{2m_W}, 0, 0, \frac{m_B^2 - m_W^2}{2m_W} \right) \tag{4.5}$$

In light cone representation, we can write as

$$P_B^\mu = \frac{1}{\sqrt{2}}(m_B, m_B, 0) \tag{4.6}$$

$$q^\mu = \left(0, \frac{m_W^2 - m_B^2}{m_W}, 0 \right) \tag{4.7}$$

B meson is made up of $\bar{b}$ and u quark. The total momentum is split between both of them. The u quark mass is $0.001 GeV \sim \mathcal{O}(\Lambda_{\text{QCD}})$
So the mass hierarchy is given as

$$m_W \sim m_b \gg \Lambda_{\text{QCD}}$$

4.2 Tree Level Amplitude

There are three possible tree level diagrams for the decay. The leading order contribution only comes from Fig 4.1 (a). Other two diagrams are suppressed by $\mathcal{O}(1/m_b)$ and $\mathcal{O}(1/m_W^2)$ respectively .The Feynman amplitude of leading order diagram can be written as

$$\mathcal{M}^{(0)} = \frac{e_u e^2 V_{ub}}{4\sqrt{2}\sin\theta_W} \left(-i\frac{\epsilon_{\mu\nu\alpha\beta}v^\mu n_-^\nu \varepsilon_W^\alpha \varepsilon_\gamma^{*\beta}}{v^+} + \varepsilon_W \cdot \varepsilon_\gamma^* \right) \int_0^\infty \frac{d\omega}{\omega} \delta\left(k^+/v^+ - \omega \right) \tag{4.8}$$

one can get the Leading order level hard kernel as following

$$T^{(0)}(\omega) = \frac{e_u e^2 V_{ub}}{4\sqrt{2}\sin\theta_W} \left(-i\frac{\epsilon_{\mu\nu\alpha\beta}P^\mu q^\nu \varepsilon_W^\alpha \varepsilon_\gamma^{*\beta}}{P \cdot q} + \varepsilon_W \cdot \varepsilon_\gamma^* \right) \frac{1}{\omega} \tag{4.9}$$
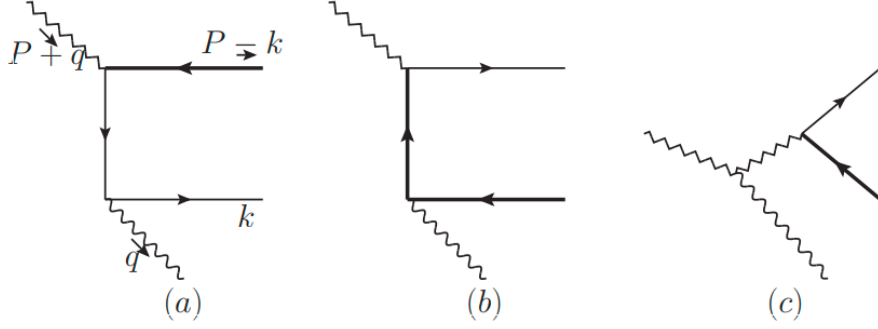
Figure 4.1: Possible Feynman diagram at tree level
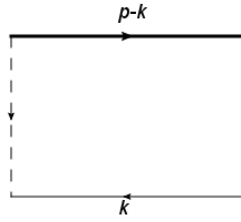
Figure 4.2: LCDA at tree level

For factorization to be valid, the hard scattering kernel must be independent of the IR effects of initial state [16]. So we can choose any state according to our own convenience. The fock space expansion of B meson is given as [19]

$$|B\rangle = |\bar{b}q\rangle + |\bar{b}gq\rangle + \dots$$

The same hard kernel is associated to all fock states. Now we can calculate form factors at LO by comparing the tree level convolution with hadronic matrix amplitude.

$$F_A^{(0)} = F_V^{(0)} = \hat{f}_B m_B \int_0^\infty \frac{d\omega}{\omega} \phi_B^+(\omega) = \frac{\hat{f}_B m_B}{\lambda_B} \tag{4.10}$$

The equality of these two form factors is due to the heavy quark spin symmetry.

4.3 One Loop level Amplitude

At one loop level, there are six Feynman diagrams as shown in Fig 5.3 which can contribute to NLO amplitude. The corresponding NLO LCDAs diagrams NLO to

23

QCD diagrams are shown in Fig 4.3. The final hard kernel $T^{(0)}$ from all these diagram can be expressed as [3]
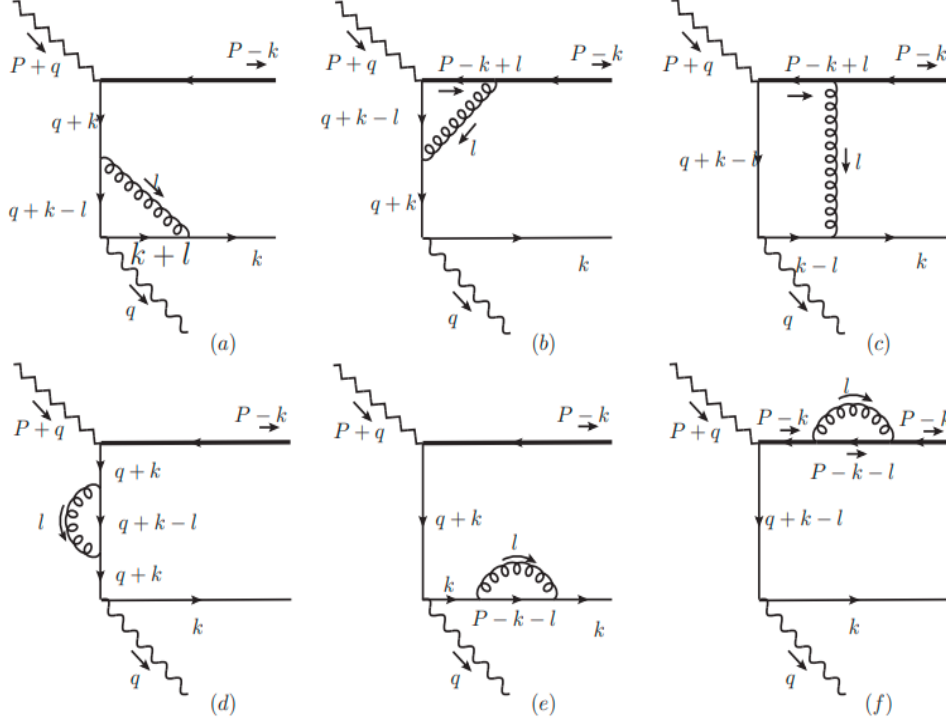
Figure 4.3: One loop QCD diagrams

$$
\begin{aligned}
T^{(1)}\left(\omega, m_b, \mu_F\right) = & \frac{\alpha_s C_F}{4\pi}\left\{\ln^2 \frac{2q^- v^+ \omega}{\mu_F^2} - 2\ln^2 \frac{m_b}{\mu_F} + \left(5 - 4\ln \frac{1-\mathrm{r}}{\mathrm{r}}\right)\ln \frac{m_b}{\mu_F}\right. \\
& + 2\operatorname{Li}_2(\mathrm{r}) + \ln^2 \mathrm{r} - \left(2\ln \frac{1-\mathrm{r}}{\mathrm{r}} - 3 + \mathrm{r}\right)\ln \frac{1-\mathrm{r}}{\mathrm{r}} + \frac{\pi^2}{12} - 7 \\
& \left. -i\pi\left[2\ln \frac{2q^- v^+ \omega}{\mu_F^2} - 4\ln \frac{m_b}{\mu_F} - \mathrm{r} - 4\ln(1-\mathrm{r}) + 2\ln \mathrm{r} + 3\right]\right\} T^{(0)}
\end{aligned}
$$

$$(4.11)$$

24
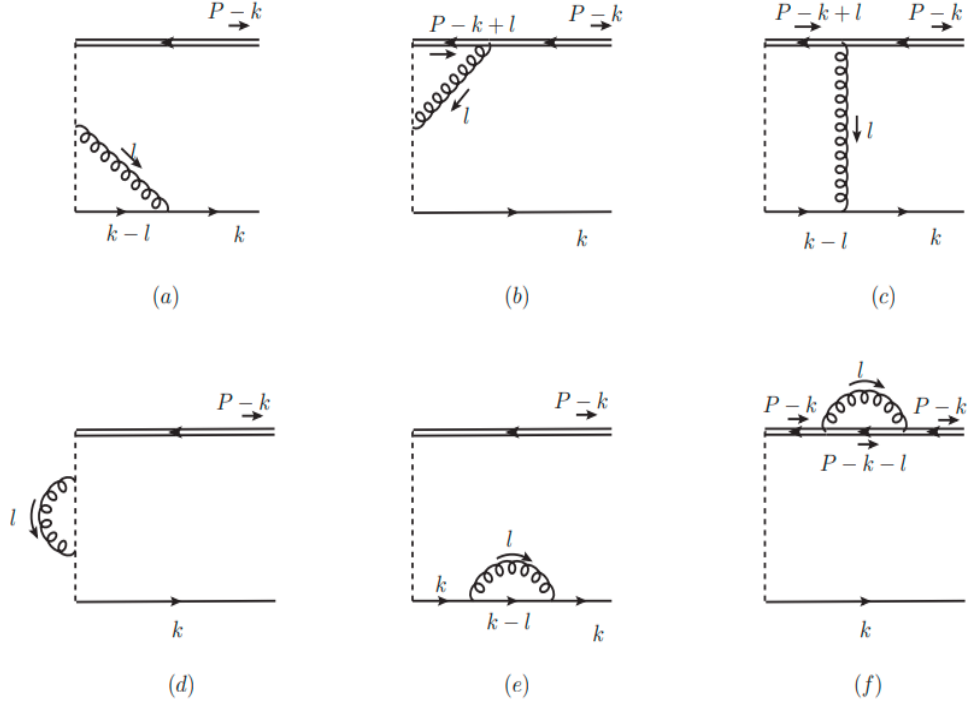
Figure 4.4: The corresponding NLO LCDAs diagrams to NLO QCD diagrams

The NLO form factors $F_{A/V}$ associated to NLO hard kernel are

$$
\begin{aligned}
F_V^{(1)} = F_A^{(1)} &= F_{V/A}^{(0)} \int_0^\infty \frac{d\omega}{\omega} \frac{T^{(1)}(\omega)}{T^{(0)}(\omega)} \phi_B^+(\omega) \\
&= F_{V/A}^{(0)} \frac{\alpha_s C_F}{4\pi} \left\{ -\ln^2 \frac{m_b}{\mu_F} - \ln \frac{m_b}{\mu_F} \left(2\ln \frac{1-r}{r} - 2 \right) + 2\operatorname{Li}_2(r) - \ln^2(1-r) \right. \\
&\quad + 2\ln r \ln(1-r) + (3-r)\ln \frac{1-r}{r} + \frac{\pi^2}{12} - 5 - 2\sigma_{B,1} \left(\ln \frac{1-r}{r} + \ln \frac{m_b}{\mu_F} \right) \\
&\quad \left. -\sigma_{B,2} + i\pi \left[2\ln \frac{m_b}{\mu_F} - 3 + r + 2\ln(1-r) + 2\sigma_{B,1} \right] \right\}
\end{aligned}
\tag{4.12}
$$

where $r \equiv m_b^2/m_W^2$, $\sigma_{B,1}$ and σ_2 are defined in Eq 3.46

Chapter 5

Factorization of the Amplitude $W^+ \rightarrow B^+ \, l^+ l^-$

In this chapter we study the factorization of the radiative decay $W^+ \rightarrow B^+ \, l^+ l^-$. There are six one loop diagrams associated to this decay at NLO. These six diagrams are solved either in HQET factorization or in QCD factorization. To check the validity of the HQET factorization for this decay, we will find out the two form factors $F_{V/A}$ to see either they are equal or not. The equality of these form factors is the validity of HQET factorization.

5.1   Kinematics of decay

As discussed in section 4.1, we can define our kinematics in either W or B frame of reference. Again both B meson and hard photon are moving in opposite direction to keep momentum conserve. The kinematics of this decay is bit different from previous decays as q^2 is no longer zero.

5.1.1   In W rest frame

Consider W boson is in rest and B meson and a virtual photon of momentum q^2 moves opposite in z axis. By using conservation of four momentum, we can write as

$$P = K - q$$

We can write the q_z of the virtual photon momentum as

$$q_z = \sqrt{E_{\gamma^*}^2 - q^2}$$

$$q_z = \sqrt{\left(\frac{m_W^2 + q^2 - m_B^2}{2m_W}\right)^2 - q^2}$$

This result can be simplified as

$$q_z = \frac{\sqrt{\lambda}}{2m_W} \tag{5.1}$$

Where $\lambda \equiv m_B^4 + \left(m_W^2 - q^2\right)^2 - 2m_B^2 \left(q^2 + m_W^2\right)$. In light cone coordinates we can write it as

$$q_W^\mu = \left(\frac{m_W^2 + q^2 - m_B^2 - \sqrt{\lambda}}{2m_W}, \frac{m_W^2 + q^2 - m_B^2 + \sqrt{\lambda}}{2m_W}, 0_\perp\right) \tag{5.2}$$

where q^2 is the momentum of virtual photon. In the limit of $q^2 = 0$, we can reproduce the results given in 4.1.1

5.1.2 In B-meson rest frame

By conservation of momentum we can write as

$$K = P + q$$

The q_z is given as

$$q_z = \sqrt{E_{\gamma^*}^2 - q^2}$$

and we can simplify the result as

$$q_z = \frac{\sqrt{\lambda}}{2m_B} \tag{5.3}$$

So we can define virtual photon momentum in light cone coordinates as

$$q_B^\mu = \left(\frac{m_W^2 - q^2 - m_B^2 - \sqrt{\lambda}}{2m_B}, \frac{m_W^2 + q^2 - m_B^2 + \sqrt{\lambda}}{2m_B}, 0_\perp\right) \tag{5.4}$$

where $\lambda \equiv m_W^4 + \left(m_B^2 - q^2\right)^2 - 2m_W^2 \left(q^2 + m_B^2\right)$. Again in the limit of $q^2 = 0$ we can reproduce the result given in 4.1.2.

5.2 HQET factorization and form factors for $W^+ \to B^+ \, l^+ l^-$

The computation of the form factors $F_{V,A}$ is conducted in the B meson's rest frame. For this, we follow the NLO calculation of $W^+ \to B^+\gamma$ [3] and therefore, it is instructive

27

to modify the HQET factorization formula reported in [3] for $W^+ \to B^+ \ell^+\ell^-$ as

$$\mathcal{M} = e\, \bar{\ell}\gamma^\mu\ell \int_0^\infty d\omega\, T_\mu(\omega, m_b, q^2, \mu_F)\Phi_B^+(\omega, \mu_F) + \mathcal{O}\left(m_b^{-1}\right), \tag{5.5}$$

$T_\mu(\omega, m_b, q^2, \mu_F)$ is hard-scattering kernel, which can be computed in perturbation theory by employing the perturbative matching technique. The hard scattering kernel is also a function of the invariant squared mass of the dilepton, q^2. In the following section, it is explicitly shown that the hard-scattering kernel for the $W \to B+\gamma$ process can be recovered by the substitution of $q^2 \to 0$ in the expression of $T_\mu(\omega, m_b, q^2, \mu_F)$. The transition amplitude $W^+ \to B^+\ l^+l^-$ transition is associated to hadronic matrix amplitude as [2]

$$\mathcal{M} = q^2\tilde{\mathcal{M}}(W^+ \to B^+\ell^+\ell^-) \tag{5.6}$$

and

$$\tilde{\mathcal{M}} = \frac{e_u e^3 V_{ub}}{4q^2\sqrt{2}\sin\theta_W}\left[\frac{\epsilon_{\mu\nu\alpha\beta}P^\nu q^\alpha \epsilon_W^\beta}{P\cdot q}F_V + i\left(\epsilon_{W\mu} + \frac{P_\mu q\cdot\epsilon_W}{P\cdot q}\right)F_A\right]\bar{\ell}\gamma^\mu\ell,$$

where e_u and e are the electric charges of spectator quark u and leptonic family respectively. V_{ub} is CKM matrix element. θ_W is week mixing angle. $F_{V/A}$ are vector and axial vector form factors which are affiliated to process $W^+ \to B^+\ l^+l^-$. The decay rate associated to the this decay in W rest frame is calculated as

$$\frac{d\Gamma}{ds\,dt} = \frac{1}{256\pi^3 m_W^3 q^4}|\mathcal{M}|^2, \tag{5.7}$$

where

$$\begin{aligned}
|\mathcal{M}|^2 =&\ \frac{(|F_V|^2 + |F_A|^2)|V_{ub}|^2}{m_W^2\left(m_B^2 - m_W^2 + s\right)^2} \times \left(\frac{2e_u^2\pi^3\alpha^3}{\sin^2\theta_W}\right) \\
&\times \Big[4m_\ell^4 s(m_B^2 + m_W^2) + 2m_\ell^2\Big(m_B^6 + m_B^4(m_W^2 + 3s) \\
&- m_B^2\big(5m_W^4 - 2m_W^2 s + s(3s + 4t)\big) + 3m_W^6 - 5m_W^4 s \\
&+ 2m_\ell^2\big(m_W^2 s(3s - 4t) - s^3\big) + 2m_B^8 \\
&- m_B^6\big(6m_W^2 + s + 2t\big) + 2t\big(m_W^6 - 3m_W^4 s + m_W^2 s^2 + s^3\big) \\
&+ m_B^4\big(6m_W^4 + m_W^2(9s + 6t) - 3s(s + 2t)\big) \\
&+ 4m_W^2 st^2 + s\big(m_W^2 - s\big)^2\big(3m_W^2 + s\big) \\
&+ m_B^2\big(-2m_W^6 - 3m_W^4(s + 2t) - 4m_W^2 st + s\big(s^2 + 6st + 4t^2\big)\big)\Big]
\end{aligned}$$

$$s_{\min} = 4m_\ell^2;$$
$$s_{\max} = (m_W - m_B)^2,$$
$$t_{\max(\min)} = \frac{1}{2}\left(2m_\ell^2 + m_B^2 + m_W^2 - s \pm \sqrt{\lambda}\sqrt{1 - \frac{4m_\ell^2}{s}}\right),$$
$$\lambda = m_B^4 - 2m_B^2 m_W^2 - 2m_B^2 s + m_W^4 - 2m_W^2 s + s^2.$$

and α is QED fine structure constant.

5.3 Factorization of tree level amplitude

There three possible diagrams associated to this decay at tree level heaving u, b quarks and W boson as the propagators as shown
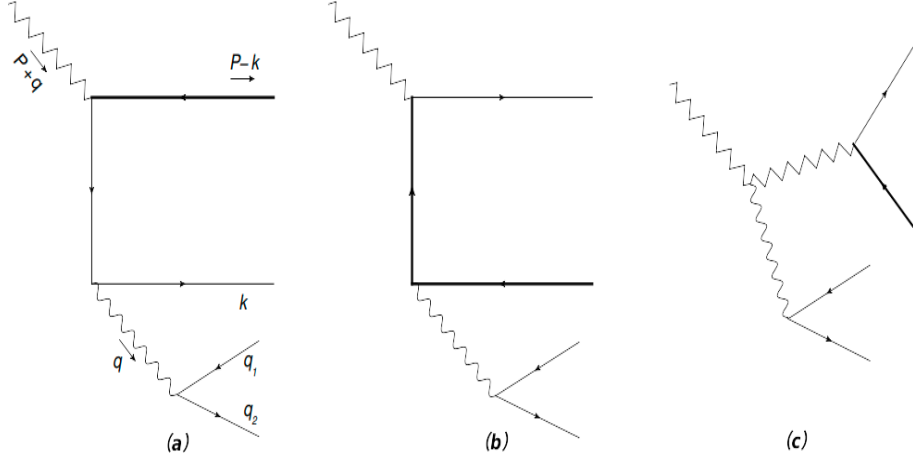
Figure 5.1: Feynman diagrams of $W^+ \to B^+ \; l^+ l^-$

The tree level amplitude associated to Fig 5.1(a) can be written as

$$\mathcal{M}^{(0)} = \frac{e_u e^2 V_{ub}}{4\sqrt{2}\sin\theta_W}\frac{\bar{u}(k)\gamma_\mu \slashed{q} \slashed{\epsilon}_W P_L \nu(p-k)}{q^2 + 2k_+ q_-}\bar{\ell}\gamma^\mu \ell \tag{5.8}$$

The LCDA diagram associated to Fig 5.1 can be simplified as

$$\Phi_{[bu]}^{\pm(0)}(\omega) = \delta\left(\frac{k^\pm}{v^\pm} - \omega\right) \tag{5.9}$$

29

Figure 5.2: Tree level LCDA diagram

By writing the amplitude in the convolution form, one can extract the tree level hard kernel as

$$T_\mu^{(0)} = \frac{e_u e^2 V_{ub}}{4\sqrt{2}\sin\theta_W} \left(-\frac{i(\epsilon_{\mu\nu\alpha\beta} p^\nu \epsilon^\alpha q^\beta)}{p\cdot q} + \epsilon_\mu + \frac{q\cdot\epsilon_W}{p\cdot q} p_\mu \right) \left(\frac{1}{\omega + q^+/v^+} \right) \qquad (5.10)$$

Analytical expression for form factors can be obtain by comparing Lorentz decomposition with factorization formula 5.5

$$F_V^{(0)} = F_A^{(0)} = f_B m_B \int_0^\infty \frac{d\omega}{\omega + q^+/v^+} \phi_B^+(\omega) = \frac{f_B m_B}{\lambda_B(q^+)} \qquad (5.11)$$
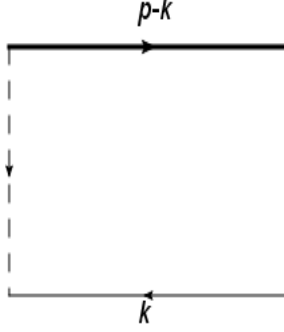
Here $\lambda_B^{-1}(q^+)$ is inverse moment of the B mesonLCDA which depends on invariant squared-mass of dilepton through $q^+ = q^2/q^-$ and defined as:

$$\frac{1}{\lambda_B(q^+)} \equiv \int_0^\infty \frac{d\omega}{\omega + q^+/v^+} \phi_B^+(\omega). \qquad (5.12)$$

5.4 NLO amplitude factorization

There are six Feynman diagrams associated to this decay at NLO. We will evaluate diagram by diagram to get the NLO hard kernel. At lower order in $1/m_b$, the dominated contribution is an order of Λ_{QCD}^{-1} that arises only through those diagrams for which the virtual photon is emitted from the spectator quark. To have the hard-scattering kernel atNLO, one needs to evaluate $\mathcal{M}^{(1)}$ in standard QCD and $\Phi^{(1)}$ in HQET.

Effective field theory general principle dictates that the infrared (IR) finite hard kernel atNLO precision can be extracted by evaluating the difference of $\mathcal{M}^{(1)}$ and $\Phi^{(1)} \otimes T_\mu^{(0)}$ on a diagram-by-diagram basis, as these quantities contain the same IR singularities. Therefore, it appears instructive to regulate mass (collinear) singularity in the same way for both $\mathcal{M}^{(1)}$ and $\Phi^{(1)} \otimes T^{(0)}$, this can be achieved by taking a nonzero mass m_u to the spectator u quark. However, dimensional regularization (with spacetime dimensions $d = 4 - 2\epsilon$) is used to regularize UV divergences. While we have used the $\overline{\text{MS}}$ renormalization scheme by redefining the 't Hooft unit mass through $\mu^2 \to \mu^2 \frac{e^{-\gamma_E}}{4\pi}$. The 't Hooft unit mass μ_R is designated for the QCD amplitude $\mathcal{M}^{(1)}$ calculation, while a different 't Hooft unit mass μ_F is used in computing $\Phi^{(1)}$.
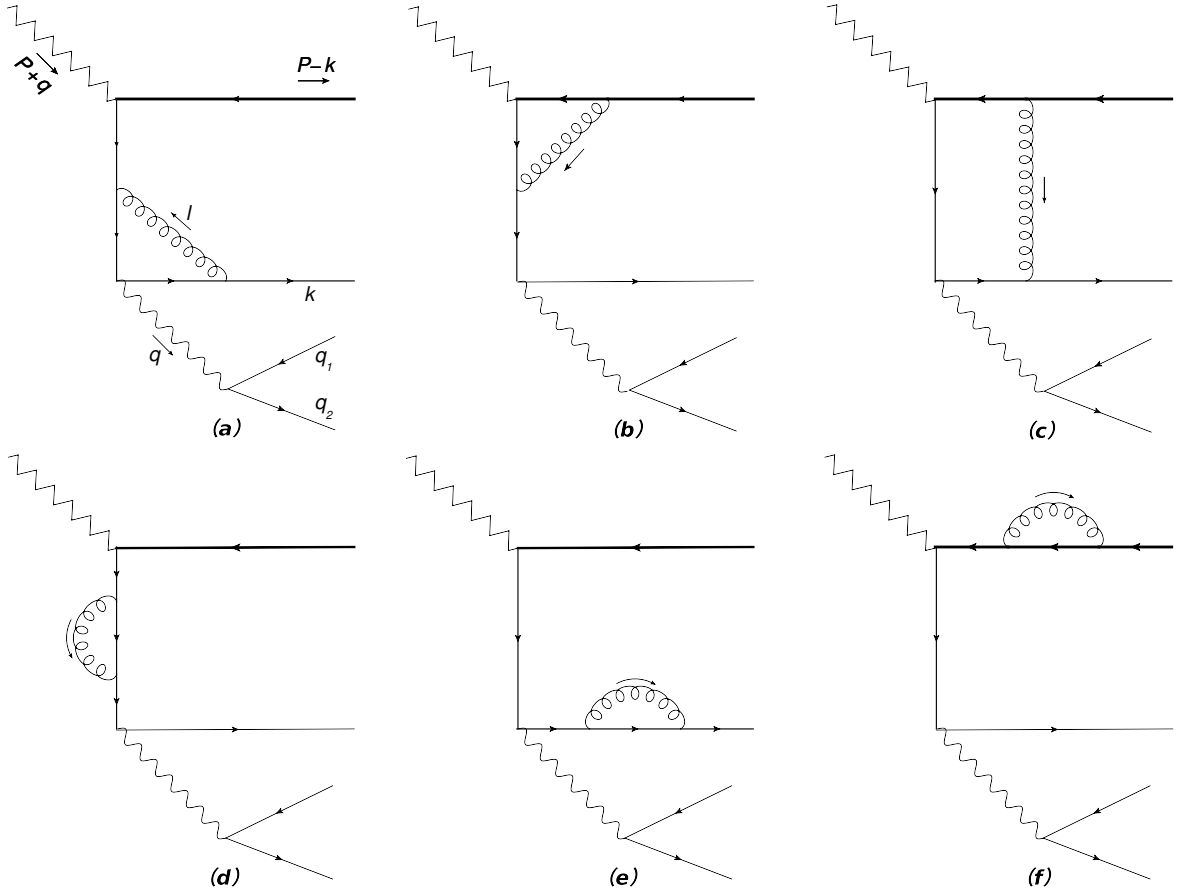

Figure 5.3: One loop Feynman amplitude diagrams to the decay $W^+ \to B^+ \ l^+ l^-$
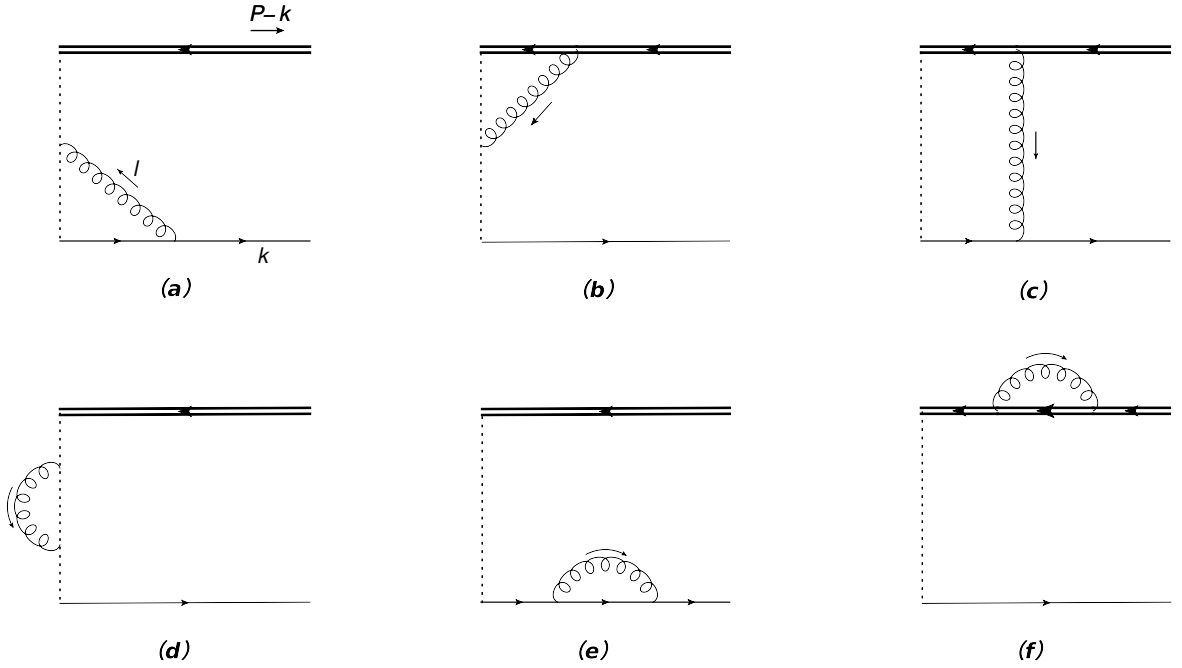
Figure 5.4: One loop LCDA diagrams to the decay $W^+ \to B^+ \ l^+l^-$

5.5   Electromagnetic Vertex Correction

The EM-QCD vertex diagram is shown in Fig 5.3(a). The associated Feynman amplitude to this diagram is

$$
\begin{aligned}
\mathcal{M}_{\mathrm{em}}^{(1)} =& \frac{\mathrm{e}_u \mathrm{e}^2 V_{ub}}{4\sqrt{2}\sin\theta_W} \int \mathrm{d}^D l \\
&\times \frac{\bar{\mathrm{u}}\gamma^\mu(\not{k}+\not{l}+\mathrm{m})\gamma^\rho(\not{k}+\not{q}+\not{l}+\mathrm{m})\gamma_\mu(\not{k}+\not{q}+\mathrm{m})\not{\epsilon}_W \mathrm{P}_L \nu}{\left[(k+l)^2-\mathrm{m}^2\right][l^2]\left[(q+k+l)^2-\mathrm{m}^2\right]\left[(q+k)^2-m^2\right]}
\end{aligned}
\tag{5.13}
$$

Where $p^2 = m_b^2$, $k^2 = m^2$ and in this decay our $q^2 \neq 0$. At leading power in $1/m_b$, the only contribution we want ti retain is $\mathcal{M}^{(1)}$ of order $\Lambda_{\mathrm{QCD}}^{-1}$,. We have considered only those diagrams where the virtual photon is emitted from the spectator quark. The contribution to $\mathcal{M}^{(1)}$ from the electromagnetic vertex correction reads

$$
\begin{aligned}
\mathcal{M}_{\mathrm{em}}^{(1)} = &\left[\frac{1}{\epsilon} + \ln\frac{q^2+z}{m^2} + \ln\frac{\mu_R^2}{m^2} + i\pi \right. \\
&\left. - \frac{q^2}{z}\ln\frac{q^2+z}{q^2}\left(3 + 2\pi^3 + i\pi^2\left\{(2\ln\pi + \ln\frac{q^2+z}{q^2}\right\}\right)\right]\mathcal{M}^{(0)},
\end{aligned}
\tag{5.14}
$$

32

where $z = 2\,q{\cdot}k$. The perturbative contributions to the $\Phi^{(1)} \otimes T^{(0)}$ can be obtained from the *soft* loop region of the electromagnetic vertex correction as depicted in Fig. 5.4(a). The einkonal vertex and propagator in feynman rules are expressed as $-ig_s T^a n_+^\mu$ and $1/p^+$, respectively. The contribution to $\Phi^{(1)}_{+\text{em}} \otimes T^{(0)}$ takes the form

$$\Phi^{(1)}_{+\text{em}} \otimes T^{(0)} = \frac{\alpha_s C_F}{4\pi}\left(\frac{2}{\epsilon} - 4\ln\frac{m}{\mu_F} + 4\right)\mathcal{M}^{(0)} \tag{5.15}$$

where μ_F is the factorization scale. One can see, as expected, both entities $\Phi^{(1)}_{+\text{em}} \otimes T^{(0)}$ and $\mathcal{M}^{(1)}_{\text{em}}$ possess same mass singularity. Moreover, we have also included quark mass counter term diagrams in order to obtain UV-finite results. Therefore the hard-scattering kernel is independent of mass singularity and can be readily found

$$T^{(1)}_{\text{em}}(\omega) = \frac{\alpha_s C_F}{4\pi}T^{(0)}(\omega)\left[\left(\ln\frac{q^2 + 2q^-v^+\omega}{\mu_F^2} + 2\ln\frac{\mu_R}{\mu_F} - 4 + i\pi\right)\right.$$
$$\left. -\frac{q^2}{2q^-v^+\omega}\ln\frac{q^2 + 2q^-v^+\omega}{q^2}\left(3 + 2\pi^3 + i\pi^2\left\{2\ln\pi + \ln\frac{q^2 + 2q^-v^+\omega}{q^2}\right\}\right)\right]$$

5.6   Spectator Quark Propagator Correction

The Feynman amplitude associated to spectator quark propagator NLO diagram as shown in Fig 5.3(d) reads

$$\mathcal{M}^{(1)}_\Sigma = \frac{\alpha C_F}{4\pi}T^{(0)}\left(\tilde{k}_+\right)\left[-\frac{1}{\varepsilon} - 1 - \ln\left(\frac{-\mu_R^2}{q^2 + 2q^-v^+\omega}\right)\right] \tag{5.16}$$

As the gluon is attached to two points of the Wilson line as shown in Fig 5.4(d), So we get $n_+^\mu n_{+\mu} = n_+^2 = 0$. So LCDA diagram is zero at NLO At NLO, we can write the factorization theorem as

$$\mathcal{M}^{(1)}_\Sigma = \Phi^{(0)} \otimes T^{(1)}_\Sigma \tag{5.17}$$

So the hard kernel is

$$T^{(1)}_\Sigma(\omega) = \frac{\alpha_s C_F}{4\pi}T^{(0)}(\omega)\left(\ln\frac{q^2 + 2q^-v^+\omega}{\mu_R^2} - 1 + i\pi\right) \tag{5.18}$$

where UV divergence $\frac{1}{\epsilon}$ is cancelled by adding the counter term in amplitude.

5.7 External light quark correction

The external quark leg correction in QCD and associated LCDA diagrams are shown in Fig 5.3 (e) and 5.4 (e) respectively. By using the on-shell subtraction scheme, we can write as

$$\mathcal{M}_u^{(1)} = \mathcal{M}^{(0)} \frac{\delta_2^u}{2}(\mu_R) \tag{5.19}$$

where $\delta_2^u = i \frac{d\Sigma_2^u}{d\slashed{k}}\Big|_{\slashed{k}=m}$.

$$\Sigma_2^u = -i \frac{\alpha C_F}{4\pi} \mu_{R,F}^{2\varepsilon} \int d^D l \frac{\gamma^\mu (k-l+m)\gamma_\mu}{[l^2]\left[(k-l)^2 - m^2\right]} \tag{5.20}$$

$$\delta_2^u = -\frac{1}{\varepsilon} + \log\left(-\frac{k^2}{m^2}\right) - 1 - \log\left(\frac{\mu^2}{m^2}\right) \tag{5.21}$$

All terms will be cancelled and only term heaving μ will survive.

$$T_{\delta Z_u}^{(1)}(\omega) = \frac{1}{2}\left[\delta Z_u(\mu_R) - \delta Z_u(\mu_F)\right] T^{(0)}(\omega) = \frac{\alpha_s C_F}{4\pi} \ln \frac{\mu_F}{\mu_R} T^{(0)}(\omega) \tag{5.22}$$

NLO hard kernel is independent of IR singularities and depends on both re-normalization and factorization scale.

5.8 External heavy quark correction

The Feynman amplitude is calculated in QCD and LCDA is calculated in HQET factorization. Heavy quark field wave function correction and associated LCDA diagrams are shown in Fig 5.3 (f) and 5.4 (f). we can calculate hard kernel as

$$T_{\delta Z_b}^{(1)}(\omega) = \frac{1}{2}\left[\delta Z_b(\mu_R) - \delta \hat{Z}_b(\mu_F)\right] T^{(0)}(\omega) = \frac{\alpha_s C_F}{4\pi}\left(2\ln \frac{m_b}{\mu_F} + \ln \frac{m_b}{\mu_R} - 2\right) T^{(0)}(\omega)$$

5.9 Box Diagram

We can approximate the hard kernel of the box diagram via strategy of region [14]. The Fig 5.3 (c) shows the box diagram. There are four regions where the loop momentum spans and are defined as

$$\begin{aligned}
l_s^\mu &\sim \left(\Lambda_{QCD}, \Lambda_{QCD}, \Lambda_{QCD}\right) \\
l_h^\mu &\sim (m_b, m_b, m_b) \\
l_c^\mu &\sim \left(\Lambda_{QCD}, m_b, \sqrt{\Lambda_{QCD} m_b}\right) \\
l_{\bar{c}}^\mu &\sim \left(m_b, \Lambda_{QCD}, \sqrt{\Lambda_{QCD} m_b}\right)
\end{aligned} \tag{5.23}$$

Where the hard region is $\mathcal{O}(m_b)$, Soft region $\mathcal{O}(\Lambda_{QCD})$, and col-linear region $\mathcal{O}(\sqrt{\Lambda_{QCD}})$. So we can approximate the loop integral as

$$A(l) = A_h(l) + A_s(l) + A_c(l) + A_{\bar{c}}(l) \tag{5.24}$$

To apply the strategy of region, we solve loop integral in each region and then add all of them to get the final result. We will carry only leading contribution in $\mathcal{M}_{Box}$ and $\Phi_{Box} \otimes T^{(0)}$. By considering $d^4l = dl_+ dl_- dl_\perp$, the amplitude of loop integral in these four regions are

$$\begin{aligned}
\mathcal{M}^s &\sim 1/\Lambda_{QCD} \\
\mathcal{M}^h &\sim 1/m_b \\
\mathcal{M}^c &\sim 1/m_b \\
\mathcal{M}^{\bar{c}} &\sim 1/m_b
\end{aligned} \tag{5.25}$$

At the lowest order of $1/m_b$, the hard kernel $T_{Box}^{(1)} = 0$.

5.10 Weak Vertex Correction

As we have done before for electromagnetic vertex, we do the same for the weak vertex. The weak vertex QCD and counter part LCDA diagrams are shown in Fig 5.3 (b) and 5.4 (b) respectively.

5.10.1 Feynman Amplitude of Weak Vertex Correction

The QCD Feynman amplitude associated to Fig 5.3 (b) can be written as

$$\begin{aligned}
\mathrm{M}_{\mathrm{Wk}}^{(1)} ={}& \frac{1}{\epsilon} - 2\mathrm{Li}_2\left(-\frac{\mathrm{x}}{\mathrm{y}}\right) - \log\left(\frac{\mathrm{x}}{\mu_{\mathrm{R}}^2}\right) + 2\log\left(\frac{\mathrm{x}}{\mathrm{y}}\right)\log\left(\frac{\mathrm{y}}{\mathrm{z}}\right) \\
& + \frac{i\pi\mathrm{y}}{\mathrm{x}+\mathrm{y}} + 2i\pi\log\left(\frac{x}{y}+1\right) + 2\log\left(\frac{x}{y}+1\right)\log\left(\frac{y}{\mathrm{x}}\right) \\
& + \frac{\mathrm{y}\log\left(\frac{\mathrm{y}}{\mathrm{x}}\right)}{x+y} - \log^2\left(\frac{\mathrm{y}}{\mathrm{z}}\right) + 2\log\left(\frac{\mathrm{y}}{\mathrm{z}}\right) + 2i\pi\log\left(\frac{\mathrm{z}}{\mathrm{y}}\right) \\
& - \frac{2\pi^2}{3} + 4i\pi
\end{aligned} \tag{5.26}$$

where $\mathrm{x} = m_b^2$ and $\mathrm{y} = 2p.q$. The convolution associated to weak vertex is

$$\Phi_w \otimes T^{(0)} = \frac{\alpha}{4\pi}C_F\mathcal{M}^{(0)}\left[2\ln^2\left(\frac{\mu_F}{\sqrt{2}k_+}\right) + \frac{3\pi^2}{4}\right] \tag{5.27}$$

35

We can get the hard kernel from the convolution as

$$
T_{\text{wk}}^{(1)}(\omega) = \frac{\alpha_s C_F}{4\pi} T^{(0)}(\omega) \left[2\ln^2 \frac{z}{\mu_F^2} - \ln^2 \frac{q^2+z}{\mu_F^2} - 2\ln \frac{q^2+z}{\mu_F^2} - 2\ln^2 \frac{m_b}{\mu_F} - 2\ln \frac{m_b}{\mu_R} \right.
$$

$$
+ 4\ln \frac{m_b}{\mu_F} \left(1 + \ln \frac{q^2+z}{z} + \ln \frac{m_b}{\sqrt{2}q^-} \right) + \ln^2 \frac{m_b}{m_b + \sqrt{2}q^-} + \frac{\pi^2}{12}
$$

$$
+ \left(2 + 4\ln \frac{q^2+z}{z} - 2\ln \frac{\sqrt{2}q^-}{m_b} \right) \ln \frac{\sqrt{2}q^-}{m_b} + 2\,\text{Li}_2 \left(\frac{m_b}{m_b + \sqrt{2}q^-} \right)
$$

$$
+ \frac{\sqrt{2}m_b q^-}{q^2 + m_b^2 + \sqrt{2}m_b q^-} \ln \frac{q^2 + \sqrt{2}m_b q^-}{m_b^2} - i\pi \left\{ 2\ln \frac{q^2+z}{\mu_F^2} - 2\ln \frac{\sqrt{2}m_b q^-}{\mu_F^2} + \right.
$$

$$
\left. \left. 2\ln \frac{m_b^2 + \sqrt{2}m_b q^-}{\sqrt{2}m_b q^-} + \frac{\sqrt{2}m_b q^- - 2q^2}{q^2 + m_b^2 + \sqrt{2}m_b q^-} \right\} \right].
$$

Now for the NLO hard kernel for this decay, We add all the hard kernels we have calculated for each diagrams and add them resulting

$$
T^{(1)} = \frac{\alpha_s C_F}{4\pi} T^{(0)}(\omega) \left[2\ln^2 \frac{z}{\mu_F^2} - \ln^2 \frac{q^2+z}{\mu_F^2} - 2\ln^2 \frac{m_b}{\mu_F} + \ln^2 \frac{m_b}{m_b + \sqrt{2}q^-} \right.
$$

$$
+ \ln \frac{m_b}{\mu_F} \left(5 + 4\ln \frac{q^2+z}{z} + 4\ln \frac{m_b}{\sqrt{2}q^-} \right) + 2\ln \frac{q^2 + \sqrt{2}m_b q^-}{\sqrt{2}m_b q^-}
$$

$$
+ \left(2 + 4\ln \frac{q^2+z}{z} - 2\ln \frac{\sqrt{2}q^-}{m_b} \right) \ln \frac{\sqrt{2}q^-}{m_b} + 2\,\text{Li}_2 \left(\frac{m_b}{m_b + \sqrt{2}q^-} \right)
$$

$$
+ \frac{\sqrt{2}m_b q^-}{q^2 + m_b^2 + \sqrt{2}m_b q^-} \ln \frac{q^2 + \sqrt{2}m_b q^-}{m_b^2} + \frac{\pi^2}{12} - 7 - i\pi \left\{ 2\ln \frac{q^2+z}{\mu_F^2} \right.
$$

$$
\left. - 2\ln \frac{\sqrt{2}m_b q^-}{\mu_F^2} + 2\ln \frac{m_b^2 + \sqrt{2}m_b q^-}{\sqrt{2}m_b q^-} + \frac{2m_b^2 + 3\sqrt{2}m_b q^-}{q^2 + m_b^2 + \sqrt{2}m_b q^-} \right\}
$$

$$
+ q^2 \left(\frac{\left(2m_b^2 + \sqrt{2}m_b q^- \right) + i\pi \left(2m_b^2 + 3\sqrt{2}m_b q^- \right)}{\sqrt{2}m_b q^- \left(q^2 + m_b^2 + \sqrt{2}m_b q^- \right)} \ln \frac{q^2 + \sqrt{2}m_b q^-}{m_b^2} \right.
$$

$$
\left. \left. + \frac{1}{z} \left(3 + 2\pi^3 - i\pi^2 \left\{ 2\ln \pi + \ln \frac{q^2+z}{q^2} \right\} \right) \ln \frac{q^2+z}{q^2} \right) \right].
$$

(5.28)

36

At leading order the NLO form factor is

$$F_V^{(1)} = F_A^{(1)} = \frac{\alpha_s C_F}{4\pi} f_B m_B \int_0^\infty \frac{\phi_B^+(\omega)}{(\omega + q^+/v^+)} \left[-\ln^2 \frac{m_b}{\mu_F} - \ln \frac{m_b}{\mu_F} \left(2\ln \frac{1-r}{r} - 2 \right) \right.$$

$$+ 2\operatorname{Li}_2(r) - \ln^2(1-r) + 2\ln r \ln(1-r) + (3-r)\ln \frac{1-r}{r} + \frac{\pi^2}{12} - 5$$

$$- 2\ln \frac{\omega + q^+/v^+}{\mu_F} \left(\ln \frac{1-r}{r} + \ln \frac{m_b}{\mu_F} \right) + 2\ln^2 \frac{\omega}{\mu_F} - \ln^2 \frac{\omega + q^+/v^+}{\mu_F}$$

$$+ i\pi \left\{ 2\ln \frac{m_b}{\mu_F} - 3 + r + 2\ln(1-r) + 2\ln \frac{\omega + q^+/v^+}{\mu_F} \right\}$$

$$- \frac{q^+}{v^+ \omega} \left[\left(\ln \frac{q^2}{\mu_F^2} - \ln \frac{m_b}{\mu_F} - \ln \frac{1-r}{r} - \ln \frac{\omega + q^+/v^+}{\mu_F} \right) \right.$$

$$\left. \left. \left(3 + 2\pi^3 + i\pi^2 \left\{ \ln \frac{q^2}{\mu_F^2} - \ln \frac{m_b}{\mu_F} - \ln \frac{1-r}{r} - \ln \frac{\omega + q^+/v^+}{\mu_F} \right\} \right) \right] \right] d\omega.$$

$$(5.29)$$

The equivalence of the form factors is due to the heavy quark spin symmetry as discussed in section 3.2 and is the proof of the validity of HQET for this decay. We have recovered the Form factors of the decay $W^+ \to B^+ \gamma$ in the limit $q^2 = 0$.

Chapter 6

Numerical Analysis

In this section, we perform numerical computations to predict the vector/axial-vector form factors associated with $W^+ \to B^+ \ell^+ \ell^-$ process. We also calculate the angular observable corresponding to the decay width i.e., branching fractions. For this purpose, we use the numerical values of input parameters from PDG,

$$\sin \theta_W = 0.481, \qquad \alpha \left(m_W/2 \right) = 1/130, \qquad m_W = 80.379 \text{ GeV}, \qquad f_B = 0.190 \text{ GeV},$$
$$|V_{ub}| = 3.67 \times 10^{-3}, \qquad m_b = 4.18 \text{ GeV}, \qquad m_B = 5.279 \text{ GeV},$$

It is worth full to mention here that our theoretical predictions are based on the Grozin-Neubert exponential model, where heavy-light meson LCDA at the initial scale $\mu_0 = 1$ GeV defined as:

$$\phi_M^+ (\omega) = \frac{\omega}{\lambda_M^2} \exp \left(-\frac{\omega}{\lambda_M} \right), \tag{6.1}$$

where M denotes the heavy-light meson, with $\lambda_B \equiv \lambda_B^+(q^+ = 0) = 0.350 \pm 0.15$ GeV. In the current study, we have calculated the leading order (LO) and next-to-leading order (NLO) QCD corrections to the form factors for the decay $W^+ \to B^+ \ell^+ \ell^-$ which are defined as $F_{V/A}^{\text{LO}} \equiv F_{V/A}^{(0)}$ and $F_{V/A}^{\text{NLO}} \equiv F_{V/A}^{(0)} + F_{V/A}^{(1)}$. The form factors $F_{V/A}^{(0)}$ and $F_{V/A}^{(1)}$ are given in Eq. (5.3) and Eq.(5.29), respectively.

One can see from these equations that the form factors clearly rely on the B meson LCDA, which demonstrates scale dependence μ_F. Therefore, to understand the variation in the vector/axial-vector form factors arising due to the factorization scale μ_F, it is essential to first know the μ_F dependence of LCDA. Consequently, one can calculate the sensitivity in the physical observables such as decay rates and branching fractions to the scale μ_F. To acheive this goal, we use the analytical solutions of Lange-Neubert evolution Equation, to obtain the form factors at desired scales as a function of invariant squared-mass of dilepton, q^2.
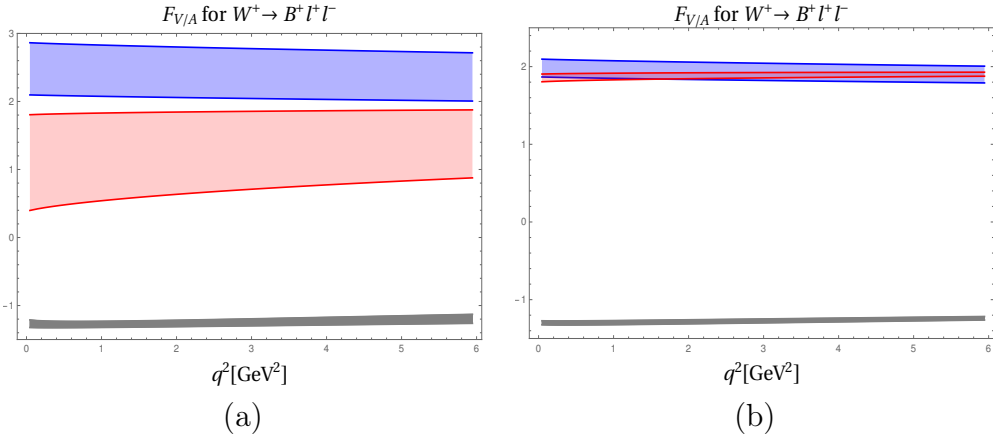
Figure 6.1: The q^2 dependence of the vector/axial vector form-factors at LO and NLO in α_s. The band represents the uncertainty from $\mu = 1$ to m_B (left) and $\mu = m_B$ to 10 GeV (right).

In Fig. 6.1, we plot the form-factors at LO and NLO in α_s as a function of q^2. The band indicates the uncertainty arising from the factorization scale, μ. We divide the variation in μ into two intervals: $1 \leq \mu_1 \leq m_B$ (left) & $m_B \leq \mu_2 \leq 10$ (right), one can notice that the q^2 dependence of the form factors is very mild for both intervals while the color bands depict the scale dependence. The blue, red and gray bands correspond to the form factors for LO ($F_{V/A}^{\mathrm{NLO}}$), real part of NLO ($\mathcal{R}e[F_{V/A}^{\mathrm{NLO}}]$) and the imaginary part of NLO ($\mathcal{I}m[F_{V/A}^{\mathrm{NLO}}]$) QCD corrections, respectively.

It is observed that these uncertainty bands of the $F_{V/A}^{\mathrm{LO}}$ and $F_{V/A}^{\mathrm{NLO}}$ (both computed at percision in α_s) turn out to be well separated as μ varies within the μ_1 interval. While for the μ_2-interval, the uncertainty bands reduce and overlap for both $F_{V/A}^{\mathrm{LO}}$ and $\mathcal{R}e[F_{V/A}^{\mathrm{NLO}}]$, however, the $\mathcal{I}m[F_{V/A}^{\mathrm{NLO}}]$ is not significantly changed. As one can also see from Fig. 6.1(b) that the reduction in the $F_{V/A}^{\mathrm{NLO}}$ is more than the $F_{V/A}^{\mathrm{LO}}$ for $m_B \leq \mu_2 \leq 10$ which is attributed to the inclusion of α_s correction in the form-factors. This ensures, the decay rates at NLO for $W^+ \to B^+ \ell^+ \ell^-$ processes in the μ_2-interval is almost insensitive as shown in Fig.6.2. However, for relatively small scales, the NLO form factors, $F_{V/A}^{\mathrm{NLO}}$, still reflect the notable dependence on μ. This residual scale dependence could be eliminated by incorporating the higher-order QCD corrections. Moreover, in our NLO predictions for decay rates, we also include the imaginary part of one loop corrections to the form factors, $\mathcal{I}m[F_{V/A}^{(1)}]$, without strictly truncating the decay width at $\mathcal{O}(\alpha_s)$. To show the μ-dependence, we have plotted the decay rates for $W^+ \to B^+ \ell^+ \ell^-$ ($\ell = e, \mu, \tau$) against μ, after integrating over $q^2 \epsilon [4m_\ell^2, 6]$ for electron and muon and $q^2 \epsilon [14, 20]$ for the tauon, in Fig. 6.2. One can notice from the graphs shown in Fig. 6.2, the LO decay rates (Γ^{LO}) strongly depend upon the μ. On the other

39

hand, the NLO decay rates (Γ^{NLO}) at low μ scale, from 1GeV to 4GeV, are highly sensitive while at relatively large scale, above than 4GeV, the sensitivity is very mild. This feature emerges due to the fact that one loop QCD corrections generate significant precision in the form factors. Consequently, the scale dependence in the NLO decay rates (Γ^{NLO}) get largely reduced, particularly, for relatively large μ. We have also calculated the numerical values of these decay rates (Γ^{LO}, Γ^{NLO}) and the branching fractions (Br^{NLO}) at NLO by varying the μ from 1Gev to 10GeV, which are listed in Tab. 6.1. We found that the NLO corrections turn to be substantial, which may vary from -75% to $+58\%$ of the LO decay rates for the case of electron and muon whereas for tauon it varies from -63% to $+71\%$. The profiles of the decay rates against the factorization scale show the similar behaviour for $W^+ \to B^+\gamma$ [3].

In addition, the theoretical predictions for the branching ratios are also influenced by the parameter $\lambda_B(\mu_0)$, because it affects the HQET factorization through ϕ_B^+. Therefore, the analysis of branching fractions as a function of λ_B is a handy tool to precisely constraint this parameter. For this purpose, to see the sensitivity of the branching fraction to the λ_B, we ploted it against the λ_B by using the range: $\lambda_B(\mu_0) = 0.35 \pm 0.15$ and shown in Fig. 6.3 by the green and red bands. Fig. 6.3(a) depicts when the leptons in the final state are electron or muon while Fig. 6.3(b) corresponds to the case of tauon as a final state leptons. The width of the green and red band represents the variation by μ in the interval $1 \leq \mu_1 \leq m_B$ and $m_B \leq \mu_2 \leq 10$, respectively.

The green band clearly indicates the strong dependence on λ_B compared to uncertainty arising from the scale μ. Similarly, the branching fraction exhibits higher sensitivity to the smaller values of λ_B compared to its larger values. Therefore, the branching fraction in the interval $m_B \leq \mu_2 \leq 10$ is more suitable to extract the precise value of λ_B, particularly, around the lower value of $\lambda_B \simeq 0.24$ GeV which is measured by Belle with 90% C.L.

Decay Channel	Γ^{LO}	Γ^{NLO}	Br^{NLO}
$W^+ \to B^+e^+e^-$	$(0.71 - 1.64) \times 10^{-11}\text{GeV}$	$(0.41 - 1.11) \times 10^{-11}\text{GeV}$	$(0.19 - 0.52) \times 10^{-11}$
$W^+ \to B^+\mu^+\mu^-$	$(0.69 - 1.61) \times 10^{-11}\text{GeV}$	$(0.40 - 1.09) \times 10^{-11}\text{GeV}$	$(0.19 - 0.52) \times 10^{-11}$
$W^+ \to B^+\tau^+\tau^-$	$(0.31 - 0.69) \times 10^{-11}\text{GeV}$	$(0.25 - 0.52) \times 10^{-11}\text{GeV}$	$(0.12 - 0.25) \times 10^{-11}$

Table 6.1. Numerical predictions to the decay rates and branching ratios for the processes $W^+ \to B^+\ell^+\ell^-$ with $\ell = e, \mu, \tau$. The uncertainty is estimated by varying μ_F from 1 GeV to 10 GeV at $\lambda_B = 0.35$ GeV after integrating over $q^2\epsilon[4m_\ell^2, 6]$ for electron and muon while for tauon integrating over $q^2\epsilon[14, 20]$.

To further explore how the parametric dependence of the branching ratio varies in the different q^2 bins, the numerical values of the branching ratios are calculated for the processes $W \to B^+\ell^+\ell^-$ where $\ell = e, \mu, \tau$ and listed in Tab. 6.2. To get the numerical values, we have integrated over three q^2 bins: $[4m_\ell^2, 0.96]$, $[4m_\ell^2, 6]$ and $[2, 6]$ for the

case of electron and muon while for the tauon, we have selected the q^2 bin above than the $c\bar{c}$ resonance region i.e, $[14, 20]$. In the first and second columns, we have listed the numerical values by setting the $\mu_{hc} = 1.5, \mu_h = 5\text{GeV}$ and $\lambda_B = 0.35$ GeV for the LO and NLO, respectively. In the remaining columns, we have given the uncertainties in the branching ratio by using the ranges of parameters: $\mu_{hc} = 1.5 \pm 0.5\text{GeV}, \mu_h = 5^{+5}_{-2.5}\text{GeV}$ and $\lambda_B = 0.35 \pm 0.15\text{GeV}$. The total uncertainty is calculated by adding the uncertainties due to the $\mu_{h,hc}$ and λ_B in quadrature.
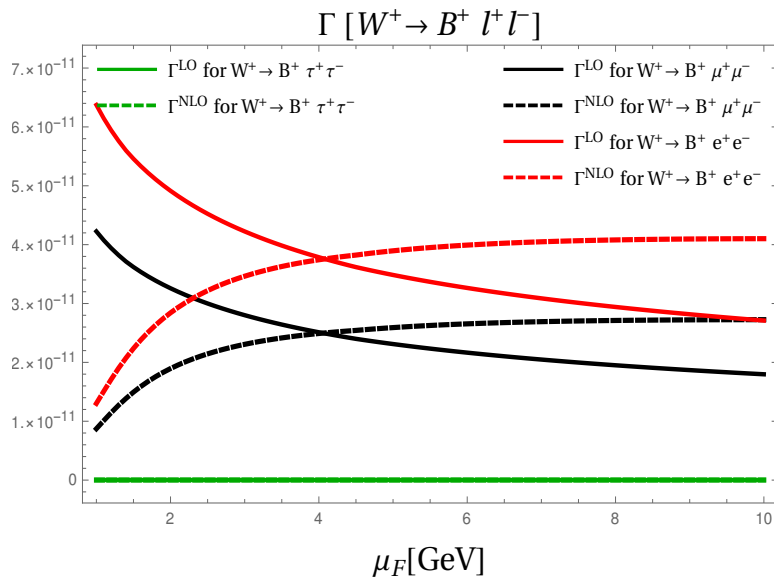

Figure 6.2: Decay rates of $W^+ \to B^+\ell^+\ell^-$ as a function of μ, which varies from 1 to 10 GeV.

41

Br$^{\text{NLO}}(W^+ \to B^+ \mu^+ \mu^-)$ Br$^{\text{NLO}}(W^+ \to B^+ \tau^+ \tau^-)$

(a)   (b)

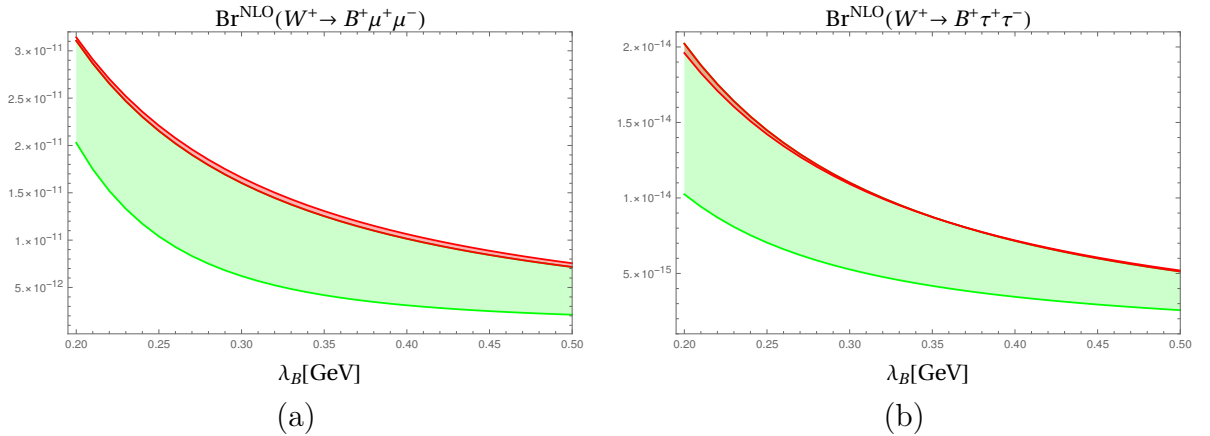Figure 6.3: Illustration of the inverse moment $\lambda_B(\mu_0)$ dependence of the branching fraction for the decay modes $W^+ \to B^+ \ell^+ \ell^-$. The uncertainly band shows the variation in μ from 1 GeV to meson mass. λ_B.

Decay	q² bin GeV²	LO $\lambda_B=0.35$ GeV (μ_{hc},μ_h)=(1.5,5)GeV	NLO $\lambda_B=0.35$ GeV (μ_{hc},μ_h)=(1.5,5)GeV	Uncertainty					
				LO (μ_{hc},μ_h)	NLO (μ_{hc},μ_h)	LO (λ_B) (1.5,5)GeV	NLO (λ_B) (1.5,5)GeV	LO (tot) (1.5,5)GeV	NLO (tot) (1.5,5)GeV
$B^+e^+e^-$	$[4m_e^2, 0.96]$	$(0.24, 0.51) \times 10^{-11}$	$(0.01, 0.17) \times 10^{-11}$	$\binom{+0.12\;+1.45}{-0.07\;-1.02}$	$\binom{+0.08\;+0.03}{-0.12\;-0.09}$	$\binom{+1.31\;+6.68}{-0.35\;-2.00}$	$\binom{+0.60\;+0.77}{-0.13\;-0.22}$	$\binom{+1.32\;+6.84}{-0.36\;-2.25}$	$\binom{+0.61\;+0.77}{-0.18\;-0.24}$
	$[4m_e^2, 6]$	$(0.14, 0.91) \times 10^{-11}$	$(0.68, 1.07) \times 10^{-11}$	$\binom{+0.70\;+0.81}{-0.42\;-0.61}$	$\binom{+0.47\;+0.11}{-0.82\;-0.47}$	$\binom{+7.57\;+3.88}{-2.05\;-1.19}$	$\binom{+3.69\;+4.75}{-0.89\;-1.40}$	$\binom{+7.60\;+3.96}{-2.09\;-1.34}$	$\binom{+3.72\;+4.75}{-1.21\;-1.49}$
	$[2, 6]$	$(0.92, 0.59) \times 10^{-11}$	$(0.46, 0.72) \times 10^{-11}$	$\binom{+0.46\;+0.53}{-0.29\;-0.39}$	$\binom{+0.31\;+0.06}{-0.55\;-0.29}$	$\binom{+4.89\;+2.51}{-1.34\;-0.78}$	$\binom{+2.44\;+3.15}{-0.60\;-0.93}$	$\binom{+4.91\;+2.57}{-1.37\;-0.87}$	$\binom{+2.46\;+3.15}{-0.81\;-0.97}$
$B^+\mu^+\mu^-$	$[4m_\mu^2, 0.96]$	$(0.21, 0.13) \times 10^{-11}$	$(0.09, 0.15) \times 10^{-11}$	$\binom{+0.11\;+0.12}{-0.06\;-0.09}$	$\binom{+0.07\;+0.02}{-0.11\;-0.08}$	$\binom{+1.14\;+0.58}{-0.30\;-0.15}$	$\binom{+0.52\;+0.67}{-0.12\;-0.19}$	$\binom{+1.15\;+0.59}{-0.31\;-0.17}$	$\binom{+0.53\;+0.67}{-0.16\;-0.21}$
	$[4m_\mu^2, 6]$	$(0.14, 0.88) \times 10^{-11}$	$(0.66, 1.04) \times 10^{-11}$	$\binom{+0.68\;+0.78}{-0.41\;-0.59}$	$\binom{+0.45\;+0.10}{-0.80\;-0.45}$	$\binom{+7.34\;+3.77}{-1.99\;-1.15}$	$\binom{+3.59\;+4.62}{-0.86\;-1.36}$	$\binom{+7.37\;+3.85}{-2.03\;-1.29}$	$\binom{+1.74\;+4.62}{-1.74\;-1.43}$
	$[2, 6]$	$(0.92, 0.59) \times 10^{-11}$	$(0.46, 0.72) \times 10^{-11}$	$\binom{+0.45\;+0.52}{-0.27\;-0.39}$	$\binom{+0.31\;+0.06}{-0.55\;-0.29}$	$\binom{+4.86\;+2.50}{-1.33\;-0.77}$	$\binom{+2.42\;+3.13}{-0.60\;-0.93}$	$\binom{+4.88\;+2.55}{-1.36\;-0.86}$	$\binom{+2.44\;+3.13}{-0.81\;-0.98}$
$B^+\tau^+\tau^-$	$[14, 20]$	$(0.59, 0.39) \times 10^{-11}$	$(0.38, 0.52) \times 10^{-11}$	$\binom{+0.28\;+0.34}{-0.14\;-0.25}$	$\binom{+0.19\;+0.00}{-0.39\;-0.14}$	$\binom{+2.79\;+1.46}{-0.82\;-0.48}$	$\binom{+1.63\;+2.07}{-0.47\;-0.65}$	$\binom{+2.80\;+1.50}{-0.83\;-0.54}$	$\binom{+1.64\;+2.07}{-0.61\;-0.66}$

Table 6.2. The numerical values of branching ratio are integrated over the different q^2 bins for the processes $W \to B^+ \ell^+ \ell^-$ where $\ell = e, \mu, \tau$. In the first and second columns, we have listed the numerical values by setting the $\mu_{hc} = 1.5$, $\mu_h = 5$ GeV and $\lambda_B = 0.35$ GeV for the LO and NLO, respectively. In the remaining columns, we have given the uncertainties in the branching ratio by using the ranges of parameters: $\mu_{hc} = 1.5 \pm 0.5$GeV, $\mu_h = 5^{+5}_{-2.5}$ GeV, and $\lambda_B = 0.35 \pm 0.15$ GeV. The total uncertainty is calculated by adding the uncertainties due to the $\mu_{h,hc}$ and λ_B in quadrature.

Chapter 7

Conclusion

In our study we have investigated the impact of NLO pertubative corrections and their numerical prediction for the of vector and axial-vector form factors in $W^+ \to B^+ \ell^+ \ell^-$. For leading order LO the form factor are $F_{V/A}^{\text{LO}} \equiv F_{V/A}^{(0)}$ and next-to-leading order NLO form factors are $F_{V/A}^{\text{LO}} \equiv F_{V/A}^{(0)} + F_{V/A}^{(1)}$. For a fixed value of μ_F, we evaluated the LO and NLO form factors as a function of q^2.

We study the production of heavy-light meson at NLO in strong coupling α_s at leading order in $1/m_b$ through semi-leptonic W boson decay in HQET factorization approach. We explicitly calculated the IR finite hard scattering kernel at NLO. It is found that both form factors are identical upto NLO which ensures the heavy-quark spin symmetry. Our results for radiative decay are extended to non-zero invariant mass square of the two lepton pair. We stress that our result agree with those of Ref. [3] in $q^2 \to 0$ limit. Along with we also presented the λ_B and factorization scale μ_F dependence of the form factors.

In addition, by using these form factors, we have calculated the decay rates and branching ratios for the processes $W \to W^+ \ell^+ \ell^-$ where $\ell = e, \mu, \tau$. Furthermore, to show the explicit dependence of the decay rates on the form factors, we have calculated their numerical values in different bins. Finally, our calculations show that the branching ratios of the above mentioned process are sensitive to the parameter λ_B. Therefore, the precise measurements of these branching ratios would be a handy tool that not only to constraints the value of parameter λ_B but also provide a fertile ground to determine its precise value.

Appendix A

Wilson Lines

A Wilson line refers to the result of taking the exponential of a line integral of the gauge field $\mathcal{A}$ taken along along certain paths C, with the integral being ordered according to the path.

$$U^C = \mathcal{P}e^{ig_s \int (dz^\mu A_\mu(z))} \tag{A.1}$$

The symbol g_s represents the strong coupling constant, whereas $\mathcal{P}$ symbolizes path ordering, a crucial concept in the context of non-commutative fields such as $A_\mu(z)$.

Let's begin by examining a scalar field $\phi(x)$ that is complex. The phase of this field is just a matter of convention. Therefore, a theory pertaining to this field should exhibit invariance when subjected to re-definitions of the kind $\phi(x) \to e^{i\alpha}\phi(x)$. Let's consider the scenario where we want to analyze the field at two distant positions x^μ and y^μ. In a local theory, the choice of convention at x^μ should be unrelated to the choice of convention at y^μ. However, how can we determine if $\phi(x) = \phi(y)$. By altering conventions, we would get

The expression

$$\phi(\mathrm{y}) - \phi(\mathrm{x}) \to e^{i\alpha(\mathrm{y})}\phi(\mathrm{y}) - e^{i\alpha(\mathrm{x})}\phi(\mathrm{x}). \tag{A.2}$$

In order to provide clear and precise comparisons between field values at various locations, an additional element is required. This prompts the establishment of a new field $W(\mathrm{x}, \mathrm{y})$ referred to as a Wilson line. This is a bi-local field that is dependent on two points. We like the transformation to be of the form

$$W(\mathrm{x}, \mathrm{y}) \to e^{i\alpha(x)}W(\mathrm{x}, \mathrm{y})e^{-i\alpha(\mathrm{y})} \tag{A.3}$$

$$PA_{\mu_1}(z_1)A_{\mu_2}(z_2) = \theta(\lambda_1 - \lambda_2)A_{\mu_1}(z_1)A_{\mu_2}(z_2) + \theta(\lambda_2 - \lambda_1)A_{\mu_2}(z_2)A_{\mu_1}(z_1) \tag{A.4}$$
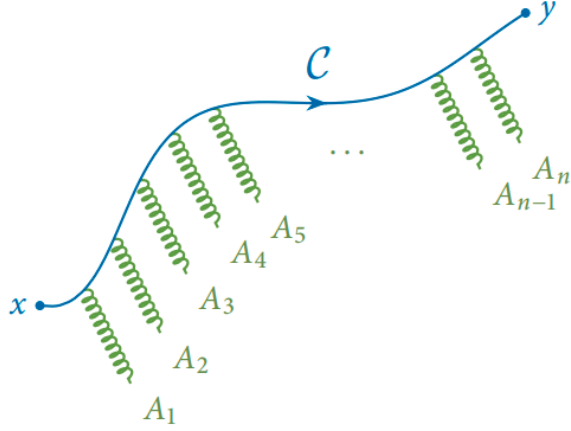
44

Figure A.1: Illustration of the term of order n in the expansion of the Wilson line, using n gluon fields that are radiating.

A.0.1 Wilson Line Feynman Rules

We begin by considering a trajectory that originates at a point a^μ and extends towards positive infinity in the direction of n^μ. The given path may be expressed as a parameterized function.

$$z^\mu = a^\mu + n^\mu \lambda \quad \lambda = 0 \ldots \infty. \tag{A.5}$$

By using path-ordering and Fourier transformation we can write as

$$I_n = (ig)^n \mu_1^{n_1} \ldots \mu_n^{n_n} e^{ia \sum k_j} \int_0^\infty \int_{\lambda_1}^\infty \ldots \int_{\lambda_{n-1}}^\infty d\lambda_1 \ldots d\lambda_n e^{i \sum (n_k; it + n_j) \lambda_j} \tag{A.6}$$
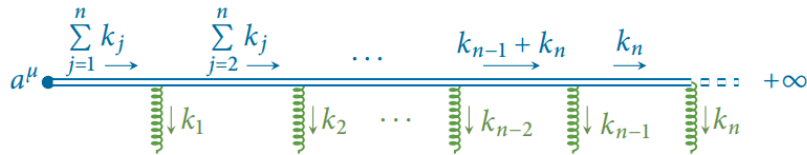

Figure A.2: The radiation of n-gluons for a Wilson line extending from a^μ to ∞

$$I_n = (ig)^n \mu_1^{n_1} \ldots \mu_n^{n_n} e^{ia \sum k_j} \prod_{j=1}^n \frac{i}{n \cdot \sum_{l=j}^n k_l + i\epsilon} \tag{A.7}$$

from above equation we can extract the Feynman rules for Wilson line.

45

- Propagator: $= \frac{i}{n \cdot k + i\epsilon}$

- Wilson line - gluon vertex: $ig n_+^\mu (t^a)_{ij}$

- Start Point: $e^{ia.k}$

- End point : $e^{-ia.k}$

Appendix B

Eikonal Approximation

The eikonal approximation assumes that moving quark emits radiation that is both soft and collinear, and this radiation may be combined into a Wilson line. In the eikonal approximation, we make the assumption that a quark has a sufficiently high momentum to disregard any changes in its momentum resulting from the emission or absorption of a low-energy soft gluon. Even after several interactions, it will not significantly depart from its original trajectory, which we consider to remain unchanged. quark of such kind is referred to as an eikonal.[8]

Consider an incoming quark of momentum p interacts with two soft gluons

$$\frac{i(\not{p} - \not{q_1} - \not{q_2})}{(p - q_1 - q_2)^2 + i\epsilon} - ig^b t^b \gamma^\nu \frac{i(\not{p} - \not{q_1})}{(p - \boldsymbol{q_1})^2 + i\epsilon} - ig^a t^a \gamma^\mu u(p) \tag{B.1}$$

under soft approximation we can neglect $\not{q_i}$

$$\frac{ip^\rho \gamma^\rho \gamma^\nu}{-2p \cdot q_1 - 2p \cdot q_2 + i\epsilon} - \frac{ig^b t^b \gamma^\rho \gamma^\nu}{-2p \cdot q_1 + i\epsilon} - ig^a t^a \gamma^\mu u(p) \tag{B.2}$$

by using anti commutation property of dirac matrices we can write it as

$$\frac{ip^\rho \gamma^\rho \gamma^\nu}{-2p \cdot q_1 - 2p \cdot q_2 + i\epsilon} - ig^b t^b \frac{ip^\sigma \{\gamma^\sigma, \gamma^\mu\}}{-2p \cdot q_1 + i\epsilon} - ig^a t^a \gamma^\mu u(p) \tag{B.3}$$

The presence of the Minkowski metric tensor in the numerator of the anti-commutator enables the representation of the quark's four momentum in the light cone basis.

$$-\frac{i}{n \cdot (q_1 + q_2) - i\epsilon} ign^\nu t^b \gamma^\nu - \frac{i}{n \cdot q_1 - i\epsilon} ign^\mu t^a \gamma^\mu u(p) \tag{B.4}$$

What we see is that the Dirac propagators have been substituted with Wilson line propagators, and the Dirac-gluon couplings have been replaced with Wilson vertices. Through the use of the eikonal approximation, we effectively separated the gluon contribution from the Dirac component.

47

Bibliography

[1] M Beneke, G Buchalla, M Neubert, and Christopher T Sachrajda. Qcd factorization for exclusive non-leptonic b-meson decays: general arguments and the case of heavy–light final states. *Nuclear Physics B*, 591(1-2):313–418, 2000.

[2] Yuval Grossman, Matthias König, and Matthias Neubert. Exclusive radiative decays of w and z bosons in qcd factorization. *Journal of High Energy Physics*, 2015(4), April 2015.

[3] Saadi Ishaq, Yu Jia, Xiaonu Xiong, and De-Shan Yang. W radiative decay to heavy-light mesons in hqet factorization through o (α s). *Physical Review D*, 100(5):054027, 2019.

[4] Feng Feng, Yu Jia, and Wen-Long Sang. Optimized predictions for $w \rightarrow b_c + \gamma$ by combining light-cone and nrqcd approaches, 2019.

[5] G Peter Lepage and Stanley J Brodsky. Exclusive processes in perturbative quantum chromodynamics. *Physical Review D*, 22(9):2157, 1980.

[6] Matthias Neubert. Aspects of qcd factorization. In *AIP Conference Proceedings*, volume 602, pages 168–179. American Institute of Physics, 2001.

[7] Matthew D Schwartz. *Quantum field theory and the standard model*. Cambridge university press, 2014.

[8] Dotcho Fakirov and Berthold Stech. F and D Decays. *Nucl. Phys. B*, 133:315–326, 1978.

[9] A. G. Grozin. Heavy quark effective theory. *Springer Tracts Mod. Phys.*, 201:1–213, 2004.

[10] Robert E. Marshak, Riazuddin, Ciaran P. Ryan, and Ernest M. Henley. Theory of Weak Interactions in Particle Physics. *Physics Today*, 24(5):48–48, 05 1971.

[11] Matthias Neubert. Heavy-quark symmetry. *Physics Reports*, 245(5–6):259–395, September 1994.

[12] Eric Braaten, Yu Jia, and Thomas Mehen. B-meson production asymmetries in perturbative qcd. *Physical Review D*, 66(3), August 2002.

[13] Mark B. Wise. Heavy quark physics, 1998.

[14] Thomas Becher, Alessandro Broggio, and Andrea Ferroglia. *Introduction to Soft-Collinear Effective Theory*. Springer International Publishing, 2015.

[15] Michael E Peskin. *An introduction to quantum field theory*. CRC press, 2018.

[16] S. Descotes-Genon and C.T. Sachrajda. Factorization, the light-cone distribution amplitude of the b-meson and the radiative decay b→. *Nuclear Physics B*, 650(1):356–390, 2003.

[17] Anne Mareike Galda and Matthias Neubert. Evolution of the b meson light-cone distribution amplitude in laplace space. *Physical Review D*, 102(7):071501, 2020.

[18] Björn O. Lange and Matthias Neubert. Renormalization-group evolution of the b-meson light-cone distribution amplitude. *Phys. Rev. Lett.*, 91:102001, Sep 2003.

[19] Gregory P Korchemsky, Dan Pirjol, and Tung-Mow Yan. Radiative leptonic decays of b mesons in qcd. *Physical Review D*, 61(11):114510, 2000.